Opiate responses are controlled by interactions of *Oprm1* and *Fgf12* loci in the murine BXD family: Correspondence to human GWAS findings

Paige M. Lemen[1], Alexander S. Hatoum[4], Price E. Dickson[2], Guy Mittleman[3], Arpana Agrawal[4], Benjamin C. Reiner[5], Wade Berrettini[5], David G. Ashbrook[1], Mustafa Hakan Gunturkun[1], Megan K. Mulligan[1], Robert W Williams[1], Hao Chen[1]

[1] University of Tennessee Health Science Center, Memphis, TN 38163 USA
[2] Marshall University, Huntington, WV 25755, USA
[3] Ball State University, Muncie IN 47306, USA
[4] Washington University, St. Louis, MO 63130, USA
[5] University of Pennsylvania, Philadelphia, PA 19104, USA

Abstract

We analyzed time-dependent behavioral responses to morphine and naloxone obtained from a large family of young adult BXD mice (*n* = 63–64 strains, including C57BL/6J and DBA/2J parents, 4–9 cases per strain) using the latest whole genome sequencing (WGS)-based genetic markers. These data include quantitative locomotor and behavior responses measured three hours after an acute morphine injection (50 mg/kg i.p.), followed by naloxone-induced withdrawal, obtained by Philip et al (2010). Locomotor data were analyzed in 15 min bins and mapped jointly for both sexes or independently for males and females. We confirmed a highly significant association between locomotor response and a genomic region that overlaps with *Oprm1* on Chr 10 at 6.8 Mb (LOD maximum of 11.4) between 15–105 min, with a peak at 75 min. Effects were modestly dependent of sex. Strains that were *B* homozygotes run 76 meters farther than those that are *D* homozygotes after a morphine injection. We discovered a novel association between a locus on Chr 16 and a late phase locomotor response (after 150 min) in both sexes. This locus had a significant but transient epistatic interaction with the *Oprm1* locus between 45–90 min, well before the main effect was detectable. The Chr 16 locus includes one compelling candidate—fibroblast growth factor 12 (*Fgf12*). Null mutation of *Fgf12* has been shown to cause locomotor deficits (e.g., ataxia). Analysis of genes correlated with both OPRM1 and FGF12 in human GWAS data of six brain regions (GTEx, v8) demonstrated an enrichment of genetic signals associated with SUD phenotypes, and a modest corroboration of variants in the *FGF12* loci on Chr 3q28. To the best of our knowledge this is the first demonstration of a transient time-dependent epistatic interaction modulating drug response in mammals—a finding with interesting mechanistic implications. Finally, this work demonstrates how high-quality FAIR+ data can be used with newly acquired data sets to yield striking results, and how joint mouse and human neurogenomic and mapping data can be merged at gene and network levels for bidirectional validation of potential SUD variants and molecular networks.

Introduction

Genetic Variation in Opioid Use Disorder

It has been challenging to discover genetic variants that influence opioid use disorder (OUD) risks in humans or in animal models (Mistry et al., 2014; Crist et al., 2019). While environmental variations clearly play a role in OUD risk, so do genetic variations (Crist et al., 2019). Classical twin studies have estimated that approximately half of the risk for OUD is genetic (Tsuang et al., 1998; Kendler et al., 2003). A few gene variants, including *KCNC1*, *KCNC2* (Gelernter et al., 2014), *CNIH3* (Nelson et al., 2016), and *RGMA* (Cheng et al., 2018) have been implicated in GWAS of OUD. A recent meta-analysis of 82,707 samples has identified the involvement of *OPRM1* (Zhou et al., 2020). Another recent study involving 41,176 samples has implicated the role of a single-nucleotide polymorphism (SNP) (rs9291211) (Polimanti et al., 2020). Most of these variants still await replication and can only explain a very small fraction of the heritability of OUD. The lack of large and adequately phenotyped human study populations is the main impediment to further discovery of specific genes (Berrettini, 2017).

The Genetic Reference Population – BXD RI Strains

Genetic mapping using model organisms, on the other hand, requires much smaller sample size, and phenotypes can be studied in greater detail. Animal models are also powerful tools for understanding the role genes play in biological processes, as well as the variation in expression of those genes. Genetic reference populations, such as recombinant inbred (RI) strains like the BXD family of mice, are useful for identifying genetic drivers responsible for trait variation and, in this case, responses to opioids. These RI strains are made by crossing two inbred strains, followed by intercrossing F1 generations, and then 20+ mating of siblings(Silver, 1995). The BXDs are the largest genetic reference population, and are made from C57BL/6J crossed with DBA/2J (referred to as B and D parental strains)(Andreux et al., 2012).

Genetic Mapping

In this study we utilize GeneNetwork, a database containing phenotypes and genotypes, and also serves as an analysis engine for quantitative trait locus (QTL) mapping, genetic correlations, and phenome-wide association studies (PheWAS) (Sloan et al., 2016; Mulligan et al., 2017; Watson and Ashbrook, 2020). QTL analysis involves connecting phenotype data with genotype data to examine genetic variation in traits controlled by multiple genes and their interaction with the environment (also called complex traits)(Lynch et al., 1998; Myles and Wayne, 2008; Goddard et al., 2016). Mapping QTL's is used to find and visualize all the chromosomal regions affecting the variation in these traits in a quantitative manner(Zeng, 2001). Over the past decade, with the expanded BXD lines, refinements in genetic markers have notably improved the possibility of detecting significant association for genotypes to phenotypes using QTL mapping and analysis; QTLs previously considered non-significant for traits might now have genome-wide significance in the larger database (Watson and Ashbrook, 2020).

In this work, we analyzed QTL's for the phenotype of locomotor response to morphine injection in the BXD family – originally collected by Philip et al. (2010). Our analysis used a new mapping algorithm recently implemented in GeneNetwork – GEMMA with LOCO (https://github.com/genetics-statistics/gemma-wrapper).GEMMA with LOCO corrects kinship (family structure) in the genotype data. We confirmed one locus on chromosome (Chr) 10 that contains *Oprm1* for early locomotor response to morphine. More importantly, we also discovered a novel locus on Chr 16 associated with the late response. *Fgf12* was a potential candidate gene in this region. Further, we found that there was a non-linear epistatic interaction (gene interaction) between these two loci.

The Importance of Epistasis

We can visualize an epistatic effect (a form of non-mendelian inheritance) on a QTL map when one position has a statistically significant interaction with another position, rather than seeing one main effect(Laurie et al., 2014). Additionally, we examine the additive effect of this interaction on locomotion and each individual haplotype of the BXD mouse line, of which epistasis is known to often produce(Wang et al., 2014). Epistasis is a fundamentally important phenomenon to study to better understand genetic pathways in complex traits and, further, the dynamics of complex genetics systems(Phillips, 2008). However, many geneticists only focus on one gene and its expression variation, ignoring the possibility of the loci interacting(Carlborg and Haley, 2004). While it is true that variation in just one gene or loci can be the underlying mechanism behind some diseases and disorders, we think it is unlikely to explain variation in complex traits such as substance use disorders (SUDs). We think this could contribute to the lack of improvements in the overdose rate, prevention, and treatment for SUDs, despite the abundant research on the role specific genes and genetics.

Translation to Humans

Lastly, we explored the possibility of translating these murine opioid response QTLs to human data and vice versa. Analysis of genes correlated with both OPRM1 and FGF12 in six human brain regions (GTEx, v8) demonstrated an enrichment of genetic signals associated with substance use disorder (SUD) phenotypes. These BXD QTLs help interpreting the results of human GWAS by providing insights into the complex interactions within the gene networks underlying the polygenic (genes interacting additively) human OUD traits.

Methods

Animal and Behavior Data Collection

Morphine-induced locomotor responses and naloxone-induced withdrawal were recorded for 64 BXD RI strains. All animals were young adults (8–9 weeks) reared at the Oak Ridge National Laboratory in 2007–2008. Detailed methods were reported in the original publication by Philip et al. (2010). Briefly, the testing protocols included receiving a single i.p. injection of morphine sulfate (50 mg/kg in isotonic saline at a volume of 10 ml/kg), followed by immediately placing the mice into an activity chamber (43.2 cm L × 43.2 cm W × 30.4 cm H, ENV-515, Med Associates, St Albans, VT, USA). Each chamber contained two sets of 16 photocells placed at 2.5 and 5 cm above the chamber floor. Activity was measured as photocell beam breaks and converted into horizontal distance traveled (cm). Horizontal distance traveled and rearing were recorded for 3 h and were exported as the sum of 15 min bins. Then, these cases received an injection of naloxone (30 mg/kg in isotonic saline at a volume of 10 ml/kg, i.p.), and were immediately returned to the chambers for an additional 15 minutes. Naloxone's effects on locomotor activity levels, and signs of withdrawal, such as the number of jumps, fecal boli, urine puddles, wet dog shakes, instances of abdominal contraction, salivation, ptosis and abnormal posture were recorded for 15 minutes.). The number of animals used per strain was 7.8 (mean ± SD) for females and 6.6 for males. Testing occurred at about 8 to 9 weeks after birth.

QTL Mapping in GeneNetwork

In this secondary analysis, phenotype data from the Philip et al. study (2010) uploaded to genenetwork.org were used. The trait IDs for the reanalysis are shown in Table 1. The Data for mapping QTLs consist of polymorphic genetic markers and quantitative trait values for strain means. Statistical heritability was also evaluated to estimate the degree of variation among the morphine and naloxone traits due to genetic variation. The original analysis by Phillip et al. (2010) was performed with the expanded BXD strain to evaluate the complementary behavioral

phenotyping using Haley-Knott regression in GeneNetwork. In our reanalysis, we first quantile normalized the trait data. We then used the newly implemented GEMMA algorithm with the LOCO option, which corrects family structure, to perform genetic mapping. Candidate genes were selected from the confidence interval of a one-LOD drop-off from the peak statistical significance as determined previously (Philip et al., 2010). The criterion for genome-wide significance was a -logP value of 5.17. Loci labeled by genetic markers could act independently at all time points or possibly in an epistatic interaction at a few time points. Therefore, we also examined epistatic interaction between two loci by performing a pair-scan, implemented in GeneNetwork (v1). This scan generated a matrix map output. Phenome-wide association studies (PheWAS) examine the relationship between a SNP and their association to collections of phenotypes. We performed a PhWAS on *Oprm1* and *Fgf12* using systems-genetics.org(Li et al., 2018).

The network for a gene of interest was defined by the top 500 genes it was correlated with in behavioral relevant brain regions in the GTEx database(GTEx Consortium et al., 2017) (e.g., substantia nigra, spinal cord, putamen, pituitary gland,hypothalamus, hippocampus, frontal cortex, cerebellum, cerebellar hemisphere, cerebellar cortex, and nucleus accumbens, etc.). Control networks were generated using additional tissues that are not likely involved in addiction (e.g., whole blood, subcutaneous tissue, transformed fibroblast cells, etc.). These networks were calculated using transcriptome data archived in GeneNetwork. Functional enrichment of these networks were obtained using WebGestalt (Zhang et al., 2005).

Human Translational Data

First, we reviewed opioid use and other relevant published GWAS data in previous literature with variants in OPRM1 and FGF12 (see results). We also extended our review to looking at potential roles of FGF12 in humans specifically. Then, All the files for FGF12 and OPRM1 correlations for each individual brain region as well as some controls were downloaded using GTExv8(GTEx Consortium et al., 2017) and GeneNetwork and then extracted out the shared genes with a liberal cut-off of 500 genes. We ran a genome-wide enrichment analysis using MAGMA, a powerful tool that identifies genes and gene-sets associated with a specific disease for analysis(de Leeuw et al., 2015). However, upon running our genome-wide enrichment analysis for OUD, we realized our initial search was too broad and much larger than in previous literature (see results). To reduce the amount of noise we identified genes that overlap between FGF12 and OPRM1 in a given tissue, and identified genes correlated specifically to each OPRM1 and FGF12 in several tissues. To do this we developed a list of genes (and Ensembl IDs) in each brain region to examine the number of occurrences each gene is seen across this data. We narrowed down our search to the top genes with high counts and compared them to the same number of genes with a count of only one. The count is the number of times the gene is found to be associated with both FGF12 and OPRM1 in all the regions/tissue datasets in GeneNetwork. Association is defined as among the top 500 genes ranked by correlation with FGF12 or OPRM1.

Results

QTL mapping of morphine induced locomotor responses

A total of 64 members of the BXD family were used in balanced male and female cohorts of roughly 6 cases per sex and strain. For details see Philip et al. (2010). The traits used in this reanalysis are shown in Table 1. Morphine induced locomotion data were recorded for 180min after morphine injection, with each 15 min dataset combined into one time bin. We first examined the distribution of the raw data (Supplementary Figure 1). Variation in locomotor responses is skewed to the right by those strains with unusually strong activation after morphine

injection. We therefore used the quantile normalized form of these data (Supplementary Figure 2) in our QTL analysis. The results of QTL mapping for each of the time bins were shown in Figure 1. The criterion for genome-wide significance was a –logP value 5.17.

During the 45–60min time interval, a significant QTL is seen on Chr 10 (at ~7.6 Mb, Figure 2a-b) in both sexes. This peak has varying $-\log_{10}P$ values of 8.59 for males and 8.39 for females. This locus contains *Oprm1*, which is likely the candidate gene. *Oprm1* encodes the mu opioid receptor (MOR). This QTL was also reported in the original analysis by Philip et al (2010). For the first 150 minutes, this peak remained as the only significant QTL, but at the morphine locomotion time frame of 150–165 minutes after injection, another significant QTL appeared on Chr 16 (~ 25–30 Mb, Figure 3a-b). The peak is larger than the previous on Chr 10, with males having a –logP of 4.64 and females –logP of 10.08. There are some possible candidate genes in this region, the most likely gene being *Fgf12*, which encodes a fibroblast growth factor 12 protein. This is a novel association that was not identified by Philip et al (2010).

Sex Differences in Peak Emergence Time

We examined the same peaks in both sexes. However, there is a slight difference in when each peak begins to emerge or disappear. In males the peak on Chr 10 begins to shrink during the 150–180 time frame, but still remains visible (Figure 1b). In females, the peak on Chr 10 has decreased during this same time frame, and is no longer visible in that time interval. There are also differences in the timing of the peak on Chr 16. In males this peak does not begin to show until 150 minutes after morphine injection. However, in females, the peak on Chr 16 begins to emerge 120 minutes after morphine injection.

To further confirm our results, we inspected the correlation (Pearson) between males and females at the highest and lowest time frames (Figure 1c-d). These figures revealed a strong positive correlation between morphine induced locomotor response and sex across the entire BXD family, with only a few noticeable outliers.

Candidate gene identification for morphine induced locomotor response

Closer examination of the QTL region on Chr 10 (Figure 2a-b), provided by visualizing maps in GeneNetwork, allows us to discover possible candidate genes in that region. Indicated by the green arrow marking the blue dots (genes), this examination shows why the candidate gene for this peak is likely *Oprm1*. MOR in the nucleus accumbens is involved in opiate-induced reward (Contet et al., 2004), and the reinforcement effect of morphine is induced by activating dopamine release from this brain region (Hyman and Malenka, 2001), so we examined *Oprm1* mRNA expression in this brain region using another dataset in GeneNetwork (Figure 2c) (Trait ID=1451709_at). Similarly, MOR signals have been observed in telencephalic nuclei, which include nucleus accumbens, striatum, amygdala, and the hippocampus (Sivalingam et al., 2020), so we checked for *Oprm1* mRNA expression in the hippocampus as well (Figure 2d) (Trait ID=5494297). This helps to validate our hypothesis that the peak on chromosome 10 is likely *Oprm1*. Further investigating, we see the list of potential candidate genes and their locations in that region (Figure 2e). The BXDs were derived from 2 fully inbred strains; C57BL/6J (B6) and DBA/2J (D2), meaning the B and D are haplotypes (Taylor et al., 1999). We generated a haplotype map in GeneNetwork to examine possible associations between these peaks and the genome of each parental strain (Figure 2f), which will be helpful for the epistatic interaction analysis later. *Oprm1* is highly polymorphic in the BXDs and variants control sensitivity to morphine locomotor response.

We also examined the second QTL, which is located on Chr 16 (Figure 3) in the latest time bin, i.e.165–180 minutes after morphine injection. This QTL is novel, with *Fgf12* as the possible candidate gene shown in the closer examination of this peak (Figure 3a-b). This gene encodes a protein that is part of the fibroblast growth factor (FGF) family. FGFs are involved in response to alcohol (Even-Chen et al., 2017) or morphine (Flores et al., 2010) in key brain

reward regions, including the striatum and ventral tegmental area (VTA). We examined striatum and VTA *Fgf12* mRNA expression to further investigate the likelihood of *Fgf12* as a potential candidate gene (Figure 3c-f). *Fgf12* has strong trans-eQTLs in BXD brain regions.

For the Chr 16 QTL, there were other potential, but less likely, candidate genes (Figure 4). These were also evaluated, but were found to be less likely the candidate for this region due to the previous literature support for *Fgf12*. To further confirm *Fgf12* as an exceptional candidate gene, we generated a Manhattan plot of the phenotypes associated with this gene (PheWAS) using systems-genetics.org(Li et al., 2018), and found that *Fgf12* significantly affects responses to various drugs, including morphine and naloxone (Figure 5).

QTL Mapping of Naloxone induced withdrawal responses

After the 180 minutes of morphine locomotion tests were complete, naloxone was injected (30 mg/kg in isotonic saline at a volume of 10 ml/kg) to induce a morphine withdrawal response. Locomotion and other behavioral measurements were taken for both males (Figure 6) and females (Figure 7). In males, a peak on chromosome 14 emerged on the QTL map for the number of jumps 0–15 minutes after naloxone injection (Figure 6a), and for the number of beam breaks (Figure 6b). Change in locomotion from before and after naloxone injection was also measured by the last 15 min of morphine locomotion response minus the first 15 min after naloxone injection (Figure 6c), which produced the same peaks on Chr 10 and 16. Salivation levels were also measured in males, producing peaks on Chr 3 and 7 (Figure 6d). The total distance traveled (horizontal activity) 0–15 minutes after naloxone injection produced peaks on Ch 14 and 12, with other less significant peaks as well (Figure 6e). Defecation in the chamber (number of fecal boli) was recorded (Figure 6f), and produces a peak on Chr 11. There are peaks on Chrs 7, 13, and 15 after the number of “wet dog shakes” (rapid and alternating head rotations) were recorded (Figure 6g). Vertical activity (rears) 0–15 minutes after naloxone injection were measured by number of beam breaks and show peaks on chromosomes 5 and 18 (figure 6h). Lastly, postural changes were recorded after naloxone injections, and peaks emerged on chromosomes 2 and 17. Each peak has their own set of potential candidate genes that could lead to a better understanding of gene expression during different time points after morphine exposure and subsequent naloxone-precipitated withdrawal.

Some withdrawal QTLs are genome-wide significant (Table 2), but more are suggestive QTLs (Supplementary Table 1). However, we chose to evaluate all potential gene candidates in the peak region on chromosome 14 of the naloxone data measuring the number of jumps 0–15min after injection in males using expression datasets in Genecup (Gunturkun et al., 2022) to see which have functional links. There are multiple candidate genes, including *Slc7a7* and *Slc7a8*. In females, peak locations were the same for total distance traveled (horizontal activity), wet dog shakes, and defecation (Figure 7c,d,f). However, for a QTL map for the number of beam breaks in females, a peak is also seen on chromosome 6 (Figure 7a). A peak is observed on chromosome 13 for vertical activity or rears (Figure7e). For salivation (Figure7g) in females, there is a peak on chromosome 16. Additionally, recordings of ptosis events (when the upper eyelid droops over the eye) reveal a peak on chromosome 2 in females only (Figure 7I).

Identifying causal variants

Using the variant browser in GeneNetwork, we asked if these QTL of *Oprm1* and *Fgf12* were expression QTLs (eQTL) caused by coding variants impacting protein structure or function, or non-coding variants impacting the transcript expression. There was no coding variant on *Fgf12* or *Oprm1* between B and D strains, all SNPs were introns. We next examined possible causal variants that were modulating expression of the candidate genes, i.e., cis-eQTLs. We checked for structural variants at the location of the *Oprm1* gene in the BXDs using linked-read sequence data in GeneNetwork and found two regions with deletions (supplementary Figure 3a-d) in the 5' UTR region of *Oprm1* on Chr 10 6.2Mb and 6.7Mb that

predicts the mRNA expression level of this gene in the striatum and hippocampus. This region has many cis-regulatory elements, but none overlap with the deletion exactly, likely because their locations are not very precise. There is a difference in expression level between the reference (orange) that shows expression in the promoter region and the homozygotic alternative (blue) that shows expression without the promoter region (deletion). We also examined three regions with deletions in the 5' UTR region of *Fgf12* on Chr16 2.74Mb, 2.76Mb and 2.77Mb with differences in mRNA expression level in the ventral tegmental area (VTA) (Supplementary Figure 3e-g) and striatum (Supplementary Figure 3h-j).

An epistatic Interaction between *Oprm1* and *Fgf12* loci modulates locomotor response to morphine

Large additive effects are detected for the locomotor responses to morphine as a function of the time after injections on Chr 10 near *Oprm1* at early time points (0–90min) and on Chr 16 near *Fgf12* in the later time periods (+90min). We hypothesize that these two loci do not act independently at all time points, but rather there is a non-linear epistatic interaction between these distinct loci even at the first time point. Figure 8 highlights this highly significant non-linear effect on locomotor activity for all four 2-locus combinations of haplotypes (combinations of the "B-maternal" and "D-paternal" haplotype for the BXDs) and individual genotypes in both sexes. The strongest epistatic effect is perceived at ~45min (Fig8c-g). The second group of strains—those that inherit the *B* haplotype on proximal Chr 10 when combined with the *D* haplotype on proximal Chr 16—have unexpectedly high levels of locomotion compared to the other three two-locus combinations. This is strong evidence of an epistatic interaction.

The full pair-scan as implemented in GeneNetwork (v1) generates the matrix map output of Figure 9a. The WebQTL implementation of the scan for 2-locus epistatic interactions is based on the DIRECT global optimization algorithm (Ljungberg et al., 2004). The strong locus at proximal Chr 10 is highlighted as a reflected reddish-colored line–one up from the x axis starting at Chr 10 and one horizontally across from Chr 10 to Chr X. This is the additive effect of the *Oprm1* region. There are two intersections of Chr 10 and Chr 16, one on each side of the diagonal. The zoomed-in region of Chr 16 on the x axis and Chr 10 on the y axis illustrates the epistatic interaction (Figure 9b). The bright red line along the bottom is the additive effect, but the vertical y axis extension of that red region reaches up to and just beyond *Fgf12* to the marker rs4170251 on Chr 16.

The pair-scan results (Supplementary Figure 4) for locomotion from **45–60** minutes shows an additive effect at the Chr 10 locus (near *Oprm1*), with a LOD of 8.46 at rs29357304 (~7.6 Mb). Results also show an additive effect at the Chr 16 locus (near *Fgf12*), with a LOD of 0.36 at rs4170251 (~32 Mb). Additive effects of both loci are above a LOD of 9.09 and the interaction effect between these two loci is a LOD of 3.52. The full model that includes all three terms has a cumulative LOD of 12.6 and is the highest LOD for a full model. The interaction effect is also significant. The Chr 10 x Chr 16 interaction is the second highest of all interactions and is the only interaction of loci that have independently significant main effects. The Chr 10 –by– Chr 16 epistatic interaction is preserved as the time window of the analysis shifts to later times. For example, mapping the locomotion from **60–75** minutes (Trait BXD_18846), gives an additive effect at the Chr 10 locus (near *Oprm1*), with a LOD of 8.21 at rs29357304 (~7.6 Mb). This timeframe also gives an additive effect at the Chr 16 locus (near *Fgf12*), with a LOD of 0.14 at rs4170251 (~32 Mb). Additive effects of both loci are above a LOD of 8.44 and the interaction effect between these two loci is a LOD of 2.97. The full model that includes all three terms has a cumulative LOD of 11.41.

At the next time window of **75**–**90** minutes (Trait BXD_18847), we report an additive effect at the Chr 10 locus (near *Oprm1*), with a LOD of 7.20 at rs29357304 (~7.6 Mb). This same timeframe also gives an additive effect at the Chr 16 locus (near *Fgf12*), with a LOD of 0.02 at rs4170251 (~32 Mb). Additive effects of both loci are above a LOD of 7.22 and the

interaction effect between these two loci has dropped to a LOD of 2.18. Together, the full model has a cumulative LOD of 9.40. In marked contrast, over the intervals from **90–105** minutes (Trait BXD_11837) and from **105–120** minutes (Trait BXD_11585), while we still detect a strong additive effect at the *Oprm1* locus with LODs of 6.73 and 5.78, respectively, we do not detect a strong epistatic interaction with Chr 16. At best, the interaction LOD is now only in the range of 1.5–2.0.

By the **120–135** minute and **150–165** minute intervals (Trait BXD_11839, and BXD_11841) even the *Oprm1* locus has faded to additive LOD scores of 2.74 and 1.15, respectively. There is no detectable interaction with the *Fgf12* locus. However, the purely additive effect at *Fgf12* is now detectible for the first time with LODs of 2.13 and 4.24, respectively. The linkage score at *Fgf12* is significant for the first time in the **150–165** minute interval (genome-wide). Finally, in the last interval—**165–180** minutes (Trait BXD_11585)—we again detect no linkage to the *Oprm1* locus, or any epistasis, but we again detect a significant additive linkage to the *Fgf12* locus with a peak LOD that has now reached 4.92.

One minor caveat in this analysis is that the implementation of the pair-scan we have used does not account for kinship among BXD family members (Ashbrook et al., 2021). However, both loci are also detected with GEMMA—a linear-mixed model mapping code that does account for kinship. Still, we chose a more conservative genome-wide significant value to account for this.

Effect of BXD epoch on morphine responses

The BXD strains we used were produced in 3 epochs (starting from 1971) . To further confirm our results, we mapped morphine response traits within each epoch (Supplemental Figure 5). We confirmed that, even with smaller sample sizes, the same additive effect on Chr 10 still existed. These results further suggested that causal variants for morphine locomotor response likely were present in the parental strains.

Human GWAS results

There is some support for these findings in human GWAS of opioid use disorder. OPRM1 variant 179971 is the only significant finding in the first well-powered meta-analysis (Zhou et al., 2020) (Hatoum et al., 2022). Another small human GWAS of opioid cessation found a signal for FGF via pathway analyses, of which *FGF12* is part (Cox et al., 2020). Full gene based results are available in the original GWAS publications.

Considering the epistatic interaction between *OPRM1* and *FGF12* and the complexity of human genetic signals, (many genes of small effects) it is possible that a network of genes in the human brain that relates to these two genes is possible. We developed a list of genes that overlap with *FGF12* and *OPRM1* in the GTEx sample (Anon, n.d.) (GTExv8). We then examined whether there is gene-based enrichment for this network via MAGMA pathway enrichment in the Zhou et al. 2020 GWAS (as this is the only publicly available sample at the time of research). Our initial analysis was performed for accumbens, putamen, caudate and adipose (as a negative control) for the FGF12 lists. This gave us only 8 tests to correct for (OUD and addiction GWAS in the four tissues). For OUD specifically, there was no significant enrichment for the original 500 gene lists, likely due to the large size of the lists and the lower power we have in SUDs GWAS. In the addiction GWAS (where FGF12 is nominally significant), there was nominal significance for putamen and caudate but not for accumbens or adipose tissue, and neither significant result passed correction for these 8 tests (p-value at ~.01).

Upon realizing that this data-set had very low power and our gene list cut-off was too large, we decided to specify our list. The network of genes was defined by examining genes correlated with OPRM1 and FGF12 found in the specific tissue (see methods). Consistent with SNP and gene-based results, there was some nominal enrichment for the addiction factor, but no enrichment for the network in the OUD GWAS (P=0.493).

While this analysis does demonstrate that the pipeline works, the lack of enrichment for the network in OUD GWAS could likely be due to the small sample size in the original human data for that specific SUD. This could also likely be due to the lack of data specification, such as the differences between examining physical dependence vs the development of OUD, initial use vs problematic use, and withdrawal vs relapse(Sanchez-Roige et al., 2021). All of these specifics across OUD stages also come with continually evolving definitions, and, therefore, also contributes to uncertainty and potential loss of significant results.

Discussion

The current opioid epidemic has generated the need for more precise and individualized treatment options for opioid use disorder (OUD). Focusing on genetics can help improve these options. BXD mice are useful for studying both the phenotypic and genetic differences in complex traits, such as OUD. They can allow us to merge human and animal genetic data at gene and network levels for bidirectional translational validation in future studies, with the hope of improving individualized treatment and prevention methods. For example, QTLs identified in the BXD strains help interpret the data of human GWAS by presenting potential chromosomal locations for contributing genes and their mechanisms for polygenic traits. During the time series that evaluated locomotor activity in mice injected with morphine, a peak on chromosome 10 is seen during the first 150 minutes. This peak links the locomotion phenotype to a region on the chromosome for where *Oprm1* is found; the well-studied gene that provides instructions for making the mu-opioid receptor (MOR). The MOR is the target of endogenous opioids such as morphine.

In the timeframe of 150–165 minutes, a strong peak on chromosome 16 appears, and we establish that the most likely candidate is *Fgf12*. *Fgf12* is part of the fibroblast growth factor (FGF) family. These growth factors regulate many biological functions, including cellular proliferation, survival, migration, and differentiation (Yun et al., 2010). Recent studies have found a correlation between the members of the FGF system and depression (Deng et al., 2019). Mouse knockout of *Fgf12* has been associated with ataxia (Goldfarb et al., 2007). There are other positional candidates, but *Fgf12* is the most biologically relevant. Elevated stress responses have been associated with a reduction in *Fgf12* in the prefrontal cortex in rats (McCreary et al., 2016). When autopsies were performed on patients with major depressive disorder, *Fgf12* was found to have increased expression in the anterior cingulate cortex (Evans et al., 2004). Variants in human *FGF12* locus have been strongly linked to the ECG PR wave intervals in a study of nearly 300 thousand subjects (Ntalla et al., 2020) and more weakly linked to cognitive decline, major depression, and sleep quality in the GWAS catalog (Burdett et al., n.d.). Distribution of the data in the plots show potential outliers (S1, S2) that may skew our results, so providing this information in the context of this study is important when making assumptions about our results. We see differences between males and females in the time courses of responses. This could be due to differences in average weight and metabolism between male and female cases, or due to the missing data for the 135–150min interval. However, further analysis is needed.

Phenotypic data were collected after naloxone injection, but peaks were not seen along a time series. Instead, peaks were seen in the behavioral data collected for chromosomes 3, 5, 7, 10, 11, 12, 13, 14, and 18. These loci are also potential novel genes that play a role in opioid abuse, warranting the need for future targeted studies to understand the relationship between these genes and their associated phenotypes. Naloxone is a potent opioid antagonist that reverses opioid overdoses (National Institute on Drug Abuse, 2021), and is often used in treatment settings or prescribed as a primary overdose prevention method (Anon, n.d.). Pharmacogenomics for both opioid agonists and antagonists has primarily focused on

individualized treatment for pain, with less priority on OUD (Wang et al., 2019). However, understanding the role genetics plays in naloxone's mechanism could initiate potentially more personalized and effective treatments for opioid abuse. Gene candidates in the peak region on chromosome 14 of data measuring the number of jumps 0–15min after injection in males were found using expression datasets in Genecup (Gunturkun et al., 2021) to see which have functional links. There are multiple candidate genes, including *Slc7a7* and *Slc7a8*. Both of these genes are a part of the solute carrier family, which play a large role in the absorption of drugs and xenobiotics (Lin et al., 2015), and are expressed in the brain. Additionally, sex differences found in other chromosomal peaks could indicate that both morphine and naloxone-precipitated withdrawal have different effects on gene expression. Similarly to the peaks shown in the morphine time series, all loci could indicate potential candidate genes with biological relevance.

Our strong evidence for an epistatic interaction among the strains that inherit the *B* haplotype on Chr 10 combined with *D* haplotype on Chr 16 come from the large additive effect and high levels of locomotion compared to the other haplotype combinations. Epistasis is often ignored as studies focus on one specific gene mutation underlying diseases (Anon, n.d.), however, complex diseases such as OUD involve both genetic and environmental factors (Anon, n.d.), and, therefore, it is important to study the interaction between different genes and loci. This study also shows the importance of time in opioid responses. Epistatic interactions aren't apparent at all time-points during the morphine-induced locomotion analysis. Instead we see the strongest effect during the middle of the test (around 75–90 min), with the peak on Chr 10 being at its highest early after morphine injection and the peak on Chr 16 at its highest at the latest time frame after morphine injection. Due to the complexity of OUD, research into the genetic susceptibility has been notoriously difficult to study, reflecting heterogeneity across comorbidities, ethnicities, environments, etc. Societal stigma and poor access to treatments inhibit the ability to collect large sample sizes. While examining epistatic interaction may complicate the findings of prior research, we propose that understanding these relationships is important in the future of preventing disease susceptibility, improving personalized medicine, and enhancing OUD treatment through pharmacogenomics and medication development.

Conclusion

In this study we confirm that the *Oprm1* locus strongly modulates the early phase locomotor response to morphine. We discovered a new locus centered on *Fgf12* that is associated with late (i.e. 165–180 min after injection) response to morphine. These two loci have a strong epistatic interaction in a short intermediate period between the early and late phases, indicating a relatively direct interaction between *Oprm1* and *Fgf12* genes or nearby alternative candidate genes. We also discovered a novel naloxone locus on Chr 14 associated for which there are two strong candidate genes—*Slc7a7* and *Slc7a8*, along with multiple other naloxone loci. Analysis of these genes in the homologous human regions and targeted analysis of the four potential candidates gives somewhat consistent evidence in sample sizes of >1 million. Thus, larger samples in human populations are needed to confirm the validity of these results.

Figure Legends

Table 1: Potential candidate genes in QTL regions that were further investigated in this study are provided. For details on any given trait, please visit the corresponding GN website by embedding the trait ID in the URL such as https://genenetwork.org/show_trait?trait_id=11845&dataset=BXDPublish (for trait BXD_11331,

Morphine response (50 mg/kg ip), locomotion (open field) from 45–60 min after injection in an activity chamber for males [cm]).

Figure 1: QTL plots for male and female of the locomotion time series after morphine injection, stacked by increasing time intervals, showing –logP values along each chromosome on the y-axis. The dotted line represents the genome-wide significance of -5.17. (a) Females. (b) Males. Strong correlation in morphine induced locomotor response between male and female BXD strains shown in a Pearson Correlation Scatterplot during the (c) 45–60min and (d) 165–180min time frames.

Figure 2: QTL map of morphine-induced locomotion with zoomed in regions for a strong peak on Chromosome 10 at *Oprm1* for the 45–60 min time interval. *Oprm1* is associated with strong cis-acting expression QTLs in several brain regions. **(a)** QTL for males with a peak –logP of 8.59 (n = 63 strains). **(b)** QTL for females a peak –logP of 8.39 (n = 64 strains). **(c)** Zoomed-in view of QTL in males. **(d)** Zoomed-in view of QTL in females. **(e)** Cis-acting expression QTL in the Nucleus Accumbens of the BXDs, with a peak –logP of 6.8 (n = 36 strains). **(f)** Cis-acting expression QTL in the Hippocampus of the BXDs, with a peak –logP 21.1 (n = 74 strains). **(g)** *Oprm1* neighborhood in BXD family with SNP densities. **(h)** Map of Haplotypes. GEMMA with LOCO was used for all association mapping.

Figure 3: QTL of morphine-induced locomotion for the late phase between 165–180 min, with zoomed in regions for the strong peak on Chr 16. This is a novel interval with *Fgf12* as a candidate gene. *Fgf12* is associated with cis-acting expression QTLs in several brain regions (a) Males with a peak –logP of 4.64 (n = 63 strains). (b) Females with a peak –logP of 10.08 (n = 64 strains), and a high *B* allele. (c) Zoomed-in view of QTL in males. (d) Zoomed-in view of QTL in females. (e) Cis-acting expression QTL in the Striatum of the BXDs, with a peak –logP of 4.38. (f) Distribution histogram and zoomed in view of region for Striatum QTL. (g) Cis-acting expression QTL in the VTA of the BXDs, with a peak –logP of 4.55. (h) Distribution histogram and zoomed in view of region VTA QTL plot. GEMMA with LOCO was used for all association mapping.

Figure 4: The late phase of 165–180min time frame QTL map, zoomed in on chromosome 16 to show genes at the peak.

Figure 5: Manhattan Plot showing *Fgf12* Phenome-Wide Association Study (PheWas) of 12 biological categories. All traits above –logP of 5.17 are of phenome-wide significance.

Figure 6: QTL of naloxone-Induced morphine withdrawal response in males. Arrow and star marks indicate the morphine locomotion peaks on chr 10 and 16. **(a)** Number of jumps 15 minutes after naloxone injection, with a –logP of 4.89 and a high B allele. **(b)** Number of beam breaks in an open field 0–15 min after naloxone injection. **(c)** Change in locomotion measured by the last 15 min of morphine locomotion response minus the first 15 min after naloxone injection. **(d)** Salivation level. **(e)** Horizontal activity (distance traveled) 0–15 min after naloxone injection. **(f)** Defecation in an activity chamber (number of fecal boli). **(g)** Wet dog shakes. **(h)**

Vertical activity (rears) 0–15 min after naloxone injection measured by number of beam breaks. **(l)** Postural change.

Figure 7: Female naloxone-induced Morphine withdrawal behavioral responses QTL maps. Arrow and star marks indicate the morphine locomotion peaks on chr 10 and 16. **(a)** Number of beam breaks during open field 0–15 min after naloxone injection. **(b)** Change in locomotion measured by the last 15 min of morphine locomotion response minus the first 15 min after naloxone injection. **(c)** Horizontal activity (distance traveled) 0–15 min after naloxone injection. **(d)** Wet dog shakes. **(e)** Vertical activity (rears) 0–15 min **(f)** Defecation in an activity chamber (number of fecal boli). **(g)** Salivation level. **(h)** Postural change. **(l)** ptosis.

Figure 8: (a) Males and **(f)** females with different combinations of the “B” or “D” haplotype yield different phenotypic results for the distance traveled over time. Distance traveled (m) between the two genotypes in **(b-e)** males and **(g-j)** females.

Figure S1: Distribution plots of the raw data for locomotion after morphine injection, both females (orange **A-K**) and males (blue **L-V**).

Figure S2: Distribution plots of the quantile normalized data for locomotion after morphine injection, both females (orange **A-K**) and males (blue **L-V**).

Figure S3: Two deletions found in the 5’ UTR region of *Oprm1* on Chr10 6.2Mb and 6.7Mb in BXD **(a-b)** striatum and **(c-d)** hippocampus. Three deletions found in the 5’ UTR region of *Fgf12* on Chr16 2.74Mb, 2.76Mb and 2.77Mb in the BXD **(e-g)** VTA and **(h-j)** striatum. The x-axis is the genotype for the deletions. The y-axis is the relative mRNA expression level. The 0/0 reference genome indicates the expression level without the deletion (orange) and the 1/1 alternative indicates the expression level without the promoter region deletion (blue).

Figure S4: (a) The two-dimensional heat map of the linkage statistics shows all pair-wise combinations of markers across the genome—both additive effects and interaction effects. A conventional genome-wide scan of the main effect is shown graphically to the far right as a single separate column. The upper left side of the diagonal is color-coded for the epistatic interaction term in the statistical model. **(b)** One of the chromosome-chromosome intersection heat maps zoomed in. The bright red line along the bottom is the additive effect.

Figure S5: (a) All Epochs (1,2,3). **(b**) Epoch 1, Trait 11845 (both sexes at 45–60 min), n = 20 strains—BXD1 to BXD32. **(c)** Epoch 3, Trait 11845 (both sexes at 45–60 min), n = 43 strains—BXD33 to BXD100. **(d)** Map of Chr 13 Trait 11845. **(e)** And the candidates in this interval of Chr 13.

References

Andreux PA, Williams EG, Koutnikova H, Houtkooper RH, Champy M-F, Henry H, Schoonjans

K, Williams RW, Auwerx J (2012) Systems genetics of metabolism: the use of the BXD murine reference panel for multiscalar integration of traits. Cell 150:1287–1299.

Anon (n.d.) GTEx Portal. Available at: https://gtexportal.org/home/gene/FGF12 [Accessed January 24, 2022a].

Anon (n.d.) Naloxone. Available at: https://www.samhsa.gov/medication-assisted-treatment/medications-counseling-related-conditions/naloxone [Accessed September 16, 2021b].

Anon (n.d.) Epistasis: Gene Interaction and Complex Disease Phenotypes. Available at: https://www.nature.com/scitable/topicpage/epistasis-gene-interaction-and-the-phenotypic-expression-907/ [Accessed September 16, 2021c].

Anon (n.d.) Complex Disease. Available at: https://www.genome.gov/genetics-glossary/Complex-Disease [Accessed September 16, 2021d].

Ashbrook DG, Arends D, Prins P, Mulligan MK, Roy S, Williams EG, Lutz CM, Valenzuela A, Bohl CJ, Ingels JF, McCarty MS, Centeno AG, Hager R, Auwerx J, Lu L, Williams RW (2021) A platform for experimental precision medicine: The extended BXD mouse family. Cell Syst 12:235–247.e9.

Berrettini W (2017) A brief review of the genetics and pharmacogenetics of opioid use disorders. Dialogues Clin Neurosci 19:229–236.

Burdett T, Hastings E, Welter D, SPOT, EMBL-EBI, NHGRI (n.d.) GWAS Catalog. Available at: https://www.ebi.ac.uk/gwas/genes/FGF12 [Accessed January 24, 2022].

Carlborg O, Haley CS (2004) Epistasis: too often neglected in complex trait studies? Nat Rev Genet 5:618–625.

Cheng Z, Zhou H, Sherva R, Farrer LA, Kranzler HR, Gelernter J (2018) Genome-wide Association Study Identifies a Regulatory Variant of RGMA Associated With Opioid Dependence in European Americans. Biol Psychiatry Available at: http://dx.doi.org/10.1016/j.biopsych.2017.12.016.

Contet C, Kieffer BL, Befort K (2004) Mu opioid receptor: a gateway to drug addiction. Curr Opin Neurobiol 14:370–378.

Cox JW, Sherva RM, Lunetta KL, Johnson EC, Martin NG, Degenhardt L, Agrawal A, Nelson EC, Kranzler HR, Gelernter J, Farrer LA (2020) Genome-Wide Association Study of Opioid Cessation. J Clin Med Res 9 Available at: http://dx.doi.org/10.3390/jcm9010180.

Crist RC, Reiner BC, Berrettini WH (2019) A review of opioid addiction genetics. Curr Opin Psychol 27:31–35.

de Leeuw CA, Mooij JM, Heskes T, Posthuma D (2015) MAGMA: generalized gene-set analysis of GWAS data. PLoS Comput Biol 11:e1004219.

Deng Z, Deng S, Zhang M-R, Tang M-M (2019) Fibroblast Growth Factors in Depression. Front Pharmacol 10:60.

Evans SJ, Choudary PV, Neal CR, Li JZ, Vawter MP, Tomita H, Lopez JF, Thompson RC,

Meng F, Stead JD, Walsh DM, Myers RM, Bunney WE, Watson SJ, Jones EG, Akil H (2004) Dysregulation of the fibroblast growth factor system in major depression. Proc Natl Acad Sci U S A 101:15506–15511.

Even-Chen O, Sadot-Sogrin Y, Shaham O, Barak S (2017) Fibroblast Growth Factor 2 in the Dorsomedial Striatum Is a Novel Positive Regulator of Alcohol Consumption. J Neurosci 37:8742–8754.

Flores JA, Galan-Rodriguez B, Rojo AI, Ramiro-Fuentes S, Cuadrado A, Fernandez-Espejo E (2010) Fibroblast growth factor-1 within the ventral tegmental area participates in motor sensitizing effects of morphine. Neuroscience 165:198–211.

Gelernter J, Kranzler HR, Sherva R, Koesterer R, Almasy L, Zhao H, Farrer LA (2014) Genome-wide association study of opioid dependence: multiple associations mapped to calcium and potassium pathways. Biol Psychiatry 76:66–74.

Goddard ME, Kemper KE, MacLeod IM, Chamberlain AJ, Hayes BJ (2016) Genetics of complex traits: prediction of phenotype, identification of causal polymorphisms and genetic architecture. Proc Biol Sci 283 Available at: http://dx.doi.org/10.1098/rspb.2016.0569.

Goldfarb M, Schoorlemmer J, Williams A, Diwakar S, Wang Q, Huang X, Giza J, Tchetchik D, Kelley K, Vega A, Matthews G, Rossi P, Ornitz DM, D'Angelo E (2007) Fibroblast growth factor homologous factors control neuronal excitability through modulation of voltage-gated sodium channels. Neuron 55:449–463.

GTEx Consortium et al. (2017) Genetic effects on gene expression across human tissues. Nature 550:204–213.

Gunturkun MH, Flashner E, Wang T, Mulligan MK, Williams RW, Prins P, Chen H (2021) GeneCup: mine PubMed for gene relationships using custom ontology and deep learning. bioRxiv:2020.09.17.297358 Available at: https://www.biorxiv.org/content/10.1101/2020.09.17.297358v5.full-text [Accessed July 12, 2021].

Gunturkun MH, Flashner E, Wang T, Mulligan MK, Williams RW, Prins P, Chen H (2022) GeneCup: mining PubMed and GWAS catalog for gene-keyword relationships. G3 Available at: http://dx.doi.org/10.1093/g3journal/jkac059.

Hatoum AS et al. (2022) Multivariate genome-wide association meta-analysis of over 1 million subjects identifies loci underlying multiple substance use disorders. bioRxiv Available at: http://medrxiv.org/lookup/doi/10.1101/2022.01.06.22268753.

Hyman SE, Malenka RC (2001) Addiction and the brain: the neurobiology of compulsion and its persistence. Nat Rev Neurosci 2:695–703.

Kendler KS, Jacobson KC, Prescott CA, Neale MC (2003) Specificity of genetic and environmental risk factors for use and abuse/dependence of cannabis, cocaine, hallucinogens, sedatives, stimulants, and opiates in male twins. Am J Psychiatry 160:687–695.

Laurie C, Wang S, Carlini-Garcia LA, Zeng Z-B (2014) Mapping epistatic quantitative trait loci. BMC Genet 15:112.

Li H et al. (2018) An Integrated Systems Genetics and Omics Toolkit to Probe Gene Function. Cell Syst 6:90–102.e4.

Lin L, Yee SW, Kim RB, Giacomini KM (2015) SLC transporters as therapeutic targets: emerging opportunities. Nat Rev Drug Discov 14:543–560.

Ljungberg K, Holmgren S, Carlborg O (2004) Simultaneous search for multiple QTL using the global optimization algorithm DIRECT. Bioinformatics 20:1887–1895.

Lynch M, Walsh B, Others (1998) Genetics and analysis of quantitative traits. Available at: http://www.invemar.org.co/redcostera1/invemar/docs/RinconLiterario/2011/febrero/AG_8.pdf.

McCreary JK, Keiko McCreary J, Sorina Truica L, Friesen B, Yao Y, Olson DM, Kovalchuk I, Cross AR, Metz GAS (2016) Altered brain morphology and functional connectivity reflect a vulnerable affective state after cumulative multigenerational stress in rats. Neuroscience 330:79–89 Available at: http://dx.doi.org/10.1016/j.neuroscience.2016.05.046.

Mistry CJ, Bawor M, Desai D, Marsh DC, Samaan Z (2014) Genetics of Opioid Dependence: A Review of the Genetic Contribution to Opioid Dependence. Curr Psychiatry Rev 10:156–167.

Mulligan MK, Mozhui K, Prins P, Williams RW (2017) GeneNetwork: A Toolbox for Systems Genetics. In: Systems Genetics: Methods and Protocols (Schughart K, Williams RW, eds), pp 75–120. New York, NY: Springer New York.

Myles C, Wayne M (2008) Quantitative trait locus (QTL) analysis. Nature Education 1 (1) 208 Available at: https://www.researchgate.net/profile/Seied-Mehdi-Miri/post/How_can_I_conduct_a_substitution_mapping/attachment/5b7c68b93843b0e6f2ab1896/AS%3A662148569112588%401534879929564/download/B+90.pdf.

National Institute on Drug Abuse (2021) Naloxone DrugFacts. Available at: https://www.drugabuse.gov/publications/drugfacts/naloxone [Accessed September 16, 2021].

Nelson EC et al. (2016) Evidence of CNIH3 involvement in opioid dependence. Mol Psychiatry 21:608–614.

Ntalla I et al. (2020) Multi-ancestry GWAS of the electrocardiographic PR interval identifies 202 loci underlying cardiac conduction. Nat Commun 11:2542.

Philip VM, Duvvuru S, Gomero B, Ansah TA, Blaha CD, Cook MN, Hamre KM, Lariviere WR, Matthews DB, Mittleman G, Goldowitz D, Chesler EJ (2010) High-throughput behavioral phenotyping in the expanded panel of BXD recombinant inbred strains. Genes Brain Behav 9:129–159.

Phillips PC (2008) Epistasis--the essential role of gene interactions in the structure and evolution of genetic systems. Nat Rev Genet 9:855–867.

Polimanti R et al. (2020) Leveraging genome-wide data to investigate differences between opioid use vs. opioid dependence in 41,176 individuals from the Psychiatric Genomics Consortium. Mol Psychiatry 25:1673–1687.

Sanchez-Roige S, Fontanillas P, Jennings MV, Bianchi SB, Huang Y, Hatoum AS, Sealock J, Davis LK, Elson SL, 23andMe Research Team, Palmer AA (2021) Genome-wide association study of problematic opioid prescription use in 132,113 23andMe research participants of European ancestry. Mol Psychiatry 26:6209–6217.

Silver LM (1995) Mouse genetics: concepts and applications. Available at: https://agris.fao.org/agris-search/search.do?recordID=US19960030675.

Sivalingam M, Ogawa S, Parhar IS (2020) Mapping of Morphine-Induced OPRM1 Gene Expression Pattern in the Adult Zebrafish Brain. Front Neuroanat 14:5.

Sloan Z, Arends D, W. Broman K, Centeno A, Furlotte N, Nijveen H, Yan L, Zhou X, W. Williams R, Prins P (2016) GeneNetwork: framework for web-based genetics. J Open Source Softw 1:25.

Taylor BA, Wnek C, Kotlus BS, Roemer N, MacTaggart T, Phillips SJ (1999) Genotyping new BXD recombinant inbred mouse strains and comparison of BXD and consensus maps. Mamm Genome 10:335–348.

Tsuang MT, Lyons MJ, Meyer JM, Doyle T, Eisen SA, Goldberg J, True W, Lin N, Toomey R, Eaves L (1998) Co-occurrence of abuse of different drugs in men: the role of drug-specific and shared vulnerabilities. Arch Gen Psychiatry 55:967–972.

Wang G, Yang E, Brinkmeyer-Langford CL, Cai JJ (2014) Additive, epistatic, and environmental effects through the lens of expression variability QTL in a twin cohort. Genetics 196:413–425.

Wang S-C, Chen Y-C, Lee C-H, Cheng C-M (2019) Opioid Addiction, Genetic Susceptibility, and Medical Treatments: A Review. Int J Mol Sci 20 Available at: http://dx.doi.org/10.3390/ijms20174294.

Watson PM, Ashbrook DG (2020) GeneNetwork: a continuously updated tool for systems genetics analyses. bioRxiv:2020.12.23.424047 Available at: https://www.biorxiv.org/content/10.1101/2020.12.23.424047v1.full [Accessed July 2, 2021].

Yun Y-R, Won JE, Jeon E, Lee S, Kang W, Jo H, Jang J-H, Shin US, Kim H-W (2010) Fibroblast growth factors: biology, function, and application for tissue regeneration. J Tissue Eng 2010:218142.

Zeng Z-B (2001) QTL Mapping. In: Brenner's Encyclopedia of Genetics (Second Edition) (Maloy S, Hughes K, eds), pp 8–12. San Diego: Academic Press.

Zhang B, Kirov S, Snoddy J (2005) WebGestalt: an integrated system for exploring gene sets in various biological contexts. Nucleic Acids Res 33:W741–W748.

Zhou H, Rentsch CT, Cheng Z, Kember RL, Nunez YZ, Sherva RM, Tate JP, Dao C, Xu K, Polimanti R, Farrer LA, Justice AC, Kranzler HR, Gelernter J, Veterans Affairs Million Veteran Program (2020) Association of OPRM1 Functional Coding Variant With Opioid Use Disorder: A Genome-Wide Association Study. JAMA Psychiatry 77:1072–1080.

Table 1: List of Potential Candidate Genes

Candidate Gene	Chromosome	Location (Mb)	Male Trait ID	Female Trait ID	Phenotype
Oprm1	Chr 10	6.788569	BXD_11331	BXD_11588	45-60min after Morphine Injection
Fgf12	Chr 16	28.157782	BXD_11328	BXD_11585	165-180min after Morphine Injection
Opa1	Chr 16	29.579333	BXD_11328	BXD_11585	165-180min after Morphine Injection
Slc7a7	Chr 14	54.369441	BXD_11336	BXD_11850	Number of Jumps After Naloxone-Induced Withdrawal
Slc7a8	Chr 14	54.722214	BXD_11336	BXD_11850	Number of Jumps After Naloxone-Induced Withdrawal

Potential candidate genes in QTL regions that were further investigated in this study are provided. For details on any given trait, please visit the corresponding GN website by embedding the trait ID in the URL such as https://genenetwork.org/show_trait?trait_id=11845&dataset=BXDPublish (for trait BXD_11331, Morphine response (50 mg/kg ip), locomotion (open field) from 45-60 min after injection in an activity chamber for males [cm]).

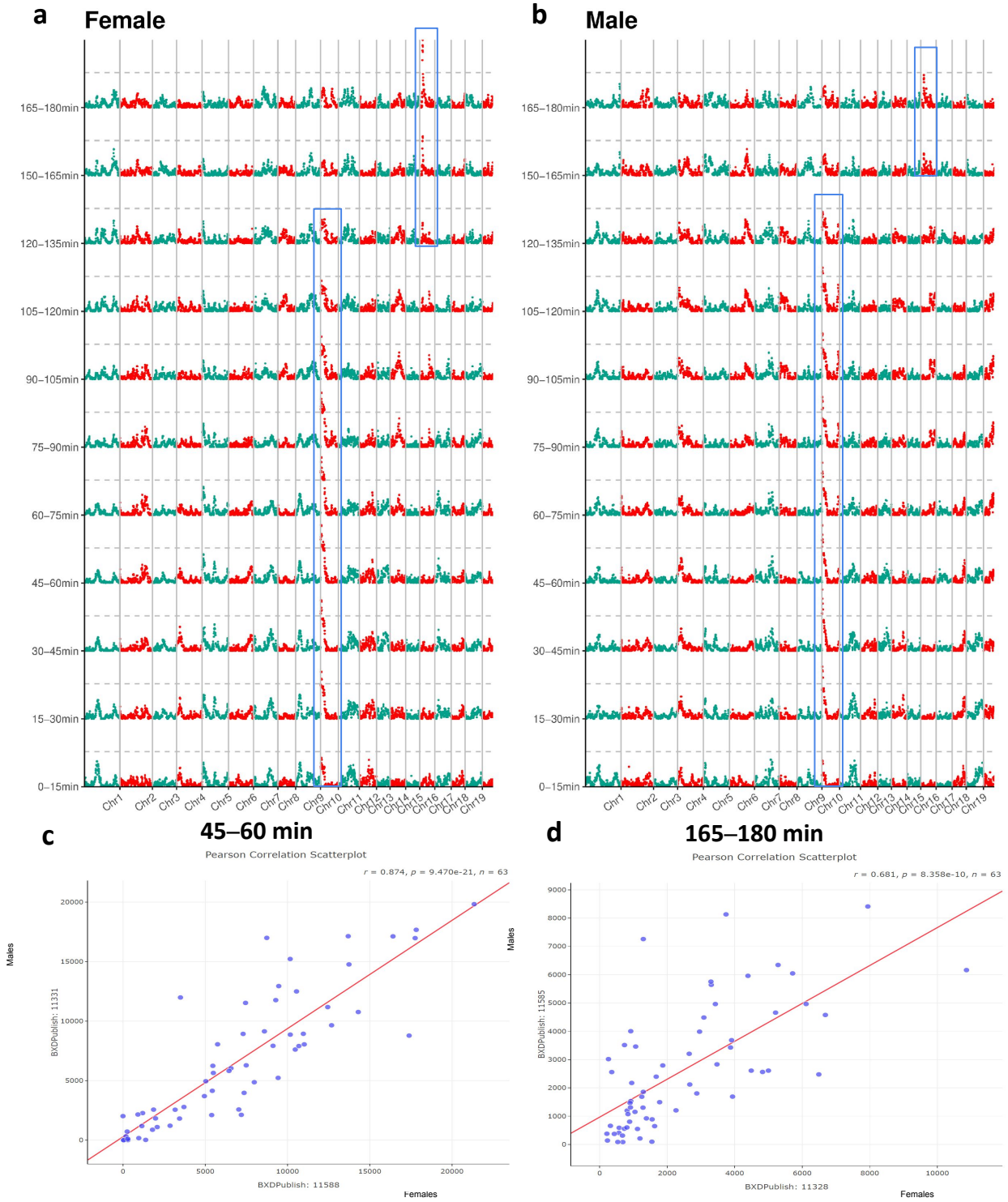

Figure 1: Stacked QTL Plots of Locomotion Time Series

QTL plots for male and female of the locomotion time series after morphine injection, stacked by increasing time intervals, showing –logP values along each chromosome on the y-axis. The dotted line represents the genome-wide significance of -5.17. **(a)** Females. **(b)** Males. Strong correlation in morphine induced locomotor response between male and female BXD strains shown in a Pearson Correlation Scatterplot during the **(c)** 45–60min and **(d)** 165–180min time frames.

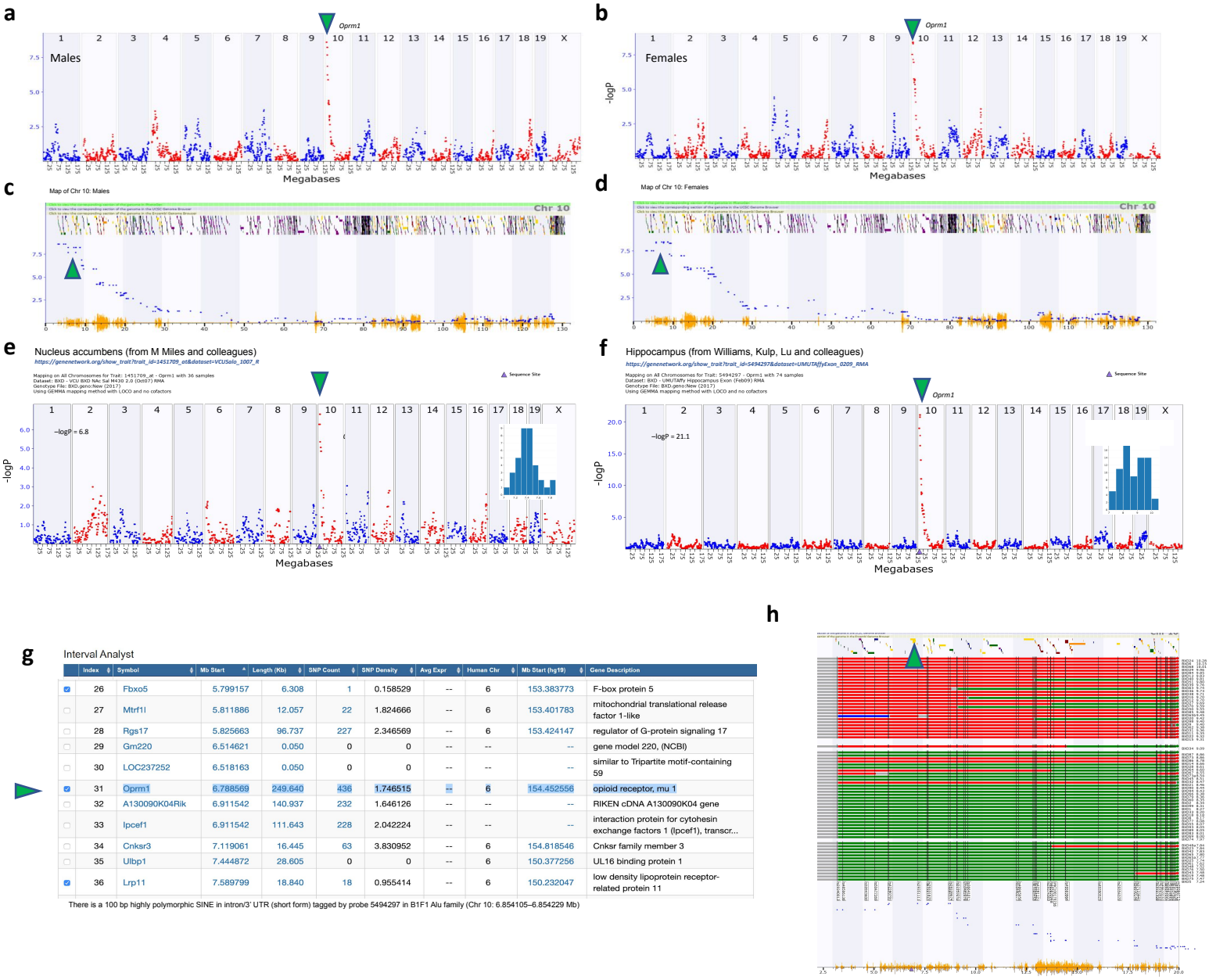

g Interval Analyst

	Index	Symbol	Mb Start	Length (Kb)	SNP Count	SNP Density	Avg Expr	Human Chr	Mb Start (hg19)	Gene Description
☑	26	Fbxo5	5.799157	6.308	1	0.158529	--	6	153.383773	F-box protein 5
☐	27	Mtrf1l	5.811886	12.057	22	1.824666	--	6	153.401783	mitochondrial translational release factor 1-like
☐	28	Rgs17	5.825663	96.737	227	2.346569	--	6	153.424147	regulator of G-protein signaling 17
☐	29	Gm220	6.514621	0.050	0	0	--	--	--	gene model 220, (NCBI)
☐	30	LOC237252	6.518163	0.050	0	0	--	--	--	similar to Tripartite motif-containing 59
☑	31	Oprm1	6.788569	249.640	436	1.746515	--	6	154.452556	opioid receptor, mu 1
☐	32	A130090K04Rik	6.911542	140.937	232	1.646126	--	--	--	RIKEN cDNA A130090K04 gene
☐	33	Ipcef1	6.911542	111.643	228	2.042224	--	--	--	interaction protein for cytohesin exchange factors 1 (Ipcef1), transcr...
☐	34	Cnksr3	7.119061	16.445	63	3.830952	--	6	154.818546	Cnksr family member 3
☐	35	Ulbp1	7.444872	28.605	0	0	--	6	150.377256	UL16 binding protein 1
☑	36	Lrp11	7.589799	18.840	18	0.955414	--	6	150.232047	low density lipoprotein receptor-related protein 11

There is a 100 bp highly polymorphic SINE in intron/3' UTR (short form) tagged by probe 5494297 in B1F1 Alu family (Chr 10: 6.854105–6.854229 Mb)

Figure 2: QTL of Morphine Locomotor at 45–60 min on Chr10

QTL map of morphine-induced locomotion with zoomed in regions for a strong peak on Chromosome 10 at *Oprm1* for the 45–60 min time interval. *Oprm1* is associated with strong cis-acting expression QTLs in several brain regions. **(a)** QTL for males with a peak –logP of 8.59 (n = 63 strains). **(b)** QTL for females a peak –logP of 8.39 (n = 64 strains). **(c)** Zoomed-in view of QTL in males. **(d)** Zoomed-in view of QTL in females. **(e)** Cis-acting expression QTL in the Nucleus Accumbens of the BXDs, with a peak –logP of 6.8 (n = 36 strains).
(f) Cis-acting expression QTL in the Hippocampus of the BXDs, with a peak –logP 21.1 (n = 74 strains).
(g) *Oprm1* neighborhood in BXD family with SNP densities. **(h)** Map of Haplotypes. GEMMA with LOCO was used for all association mapping.

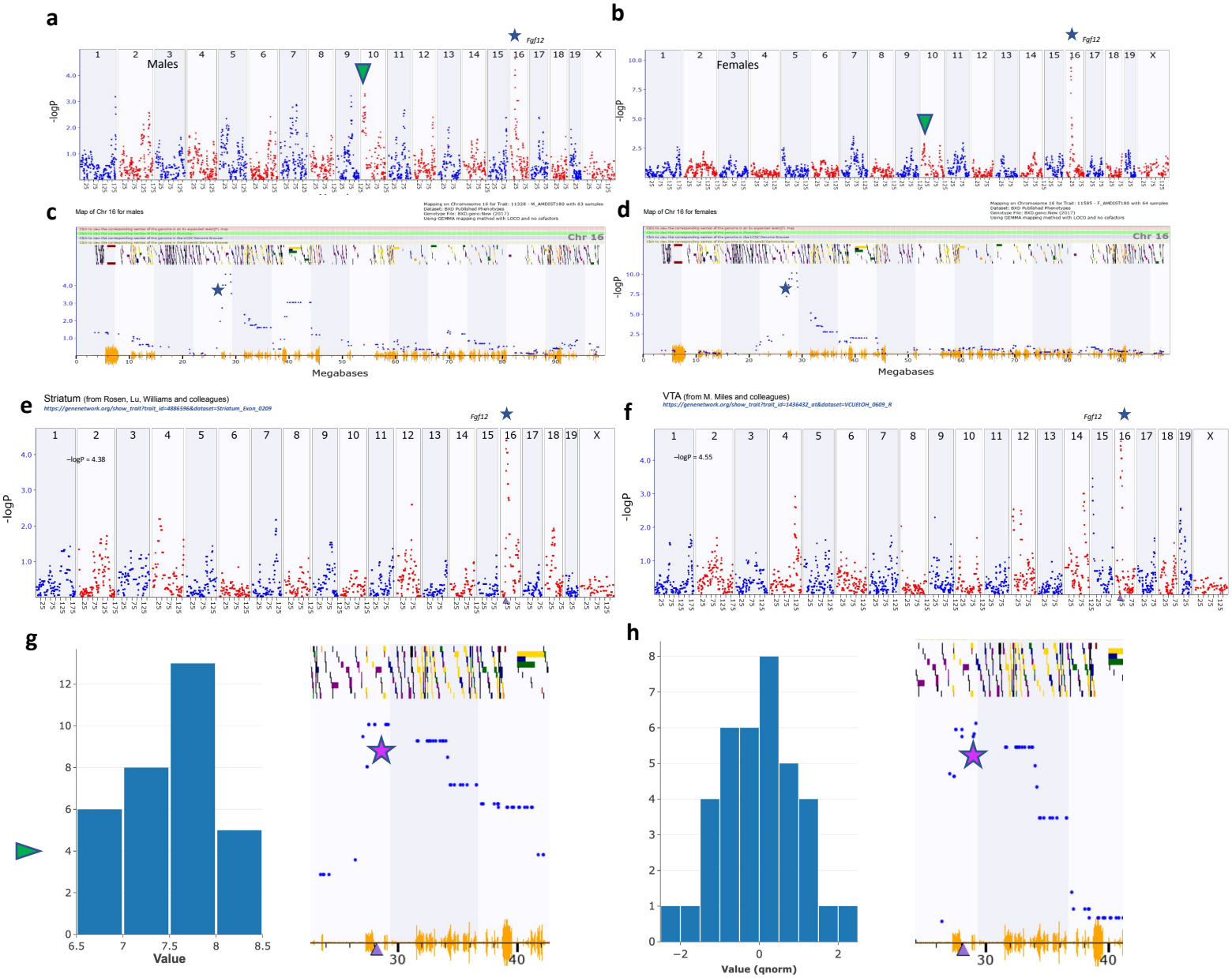

Figure 3: QTL of variation in Morphine Locomotion Between 165–180 min on Chr 16

QTL of morphine-induced locomotion for the late phase between 165–180 min, with zoomed in regions for the strong peak on Chr 16. This is a novel interval with *Fgf12* as a candidate gene. *Fgf12* is associated with cis-acting expression QTLs in several brain regions **(a)** Males with a peak –logP of 4.64 (n = 63 strains). **(b)** Females with a peak –logP of 10.08 (n = 64 strains), and a high *B* allele. **(c)** Zoomed-in view of QTL in males. **(d)** Zoomed-in view of QTL in females. **(e)** Cis-acting expression QTL in the Striatum of the BXDs, with a peak –logP of 4.38. **(f)** Distribution histogram and zoomed in view of region for Striatum QTL. **(g)** Cis-acting expression QTL in the VTA of the BXDs, with a peak –logP of 4.55. **(h)** Distribution histogram and zoomed in view of region VTA QTL plot. GEMMA with LOCO was used for all association mapping.

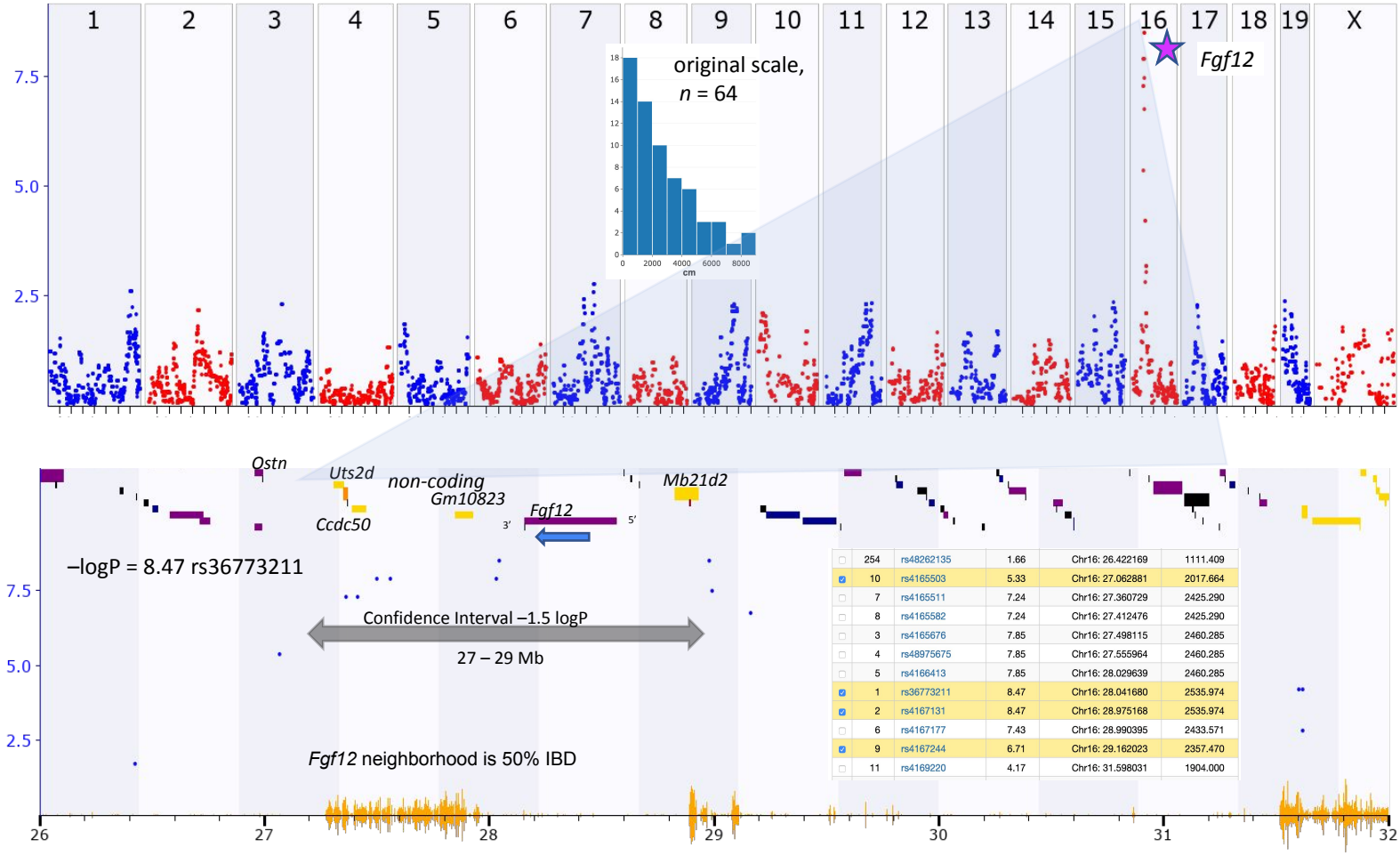

☐	254	rs48262135	1.66	Chr16: 26.422169	1111.409
☑	10	rs4165503	5.33	Chr16: 27.062881	2017.664
☐	7	rs4165511	7.24	Chr16: 27.360729	2425.290
☐	8	rs4165582	7.24	Chr16: 27.412476	2425.290
☐	3	rs4165676	7.85	Chr16: 27.498115	2460.285
☐	4	rs48975675	7.85	Chr16: 27.555964	2460.285
☐	5	rs4166413	7.85	Chr16: 28.029639	2460.285
☑	1	rs36773211	8.47	Chr16: 28.041680	2535.974
☑	2	rs4167131	8.47	Chr16: 28.975168	2535.974
☐	6	rs4167177	7.43	Chr16: 28.990395	2433.571
☑	9	rs4167244	6.71	Chr16: 29.162023	2357.470
☐	11	rs4169220	4.17	Chr16: 31.598031	1904.000

Figure 4: Late Phase Morphine — Chr 16 from 27 to 29 Mb

The late phase of 165–180min time frame QTL map, zoomed in on chromosome 16 to show genes at the peak. The effect size is 2536 cm/*B* allele

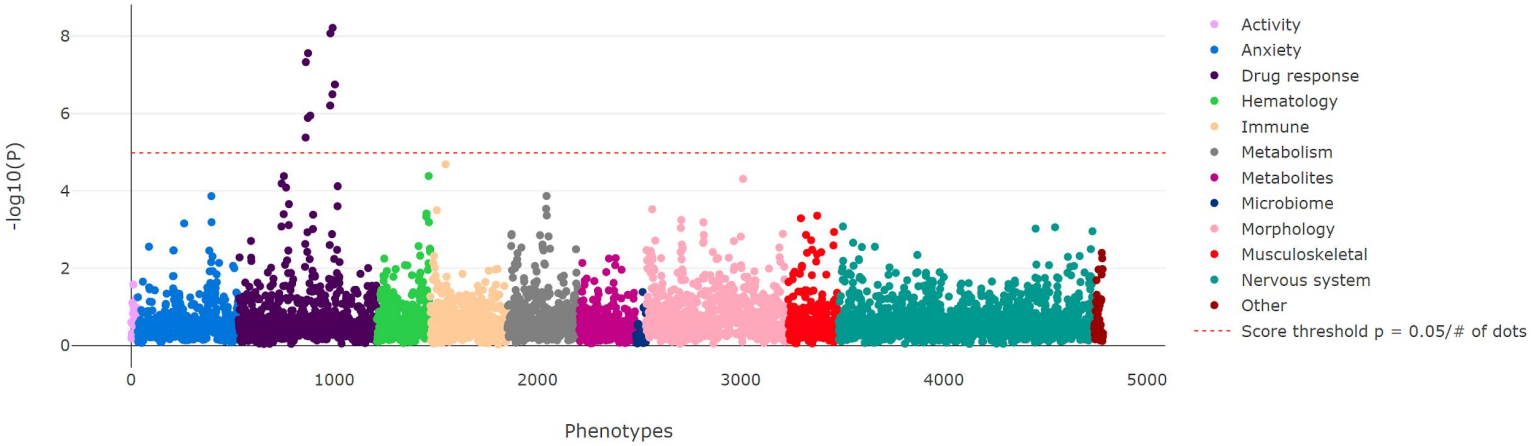

Figure 5: *Fgf12* Phenome-Wide Association Study of 12 Biological Categories

Manhattan Plot showing *Fgf12* Phenome-Wide Association Study (PheWas) of 12 biological categories. All traits above –logP of 5.17 are of phenome-wide significance.

Table 2: Genome-Wide Significant QTLs in Naloxone-Induced Withdrawal Behavior (Quantile Normalized)

Chromosome	Location (Mb)	-logP	Trait ID	Phenotype
Chr14	54.37	5.51	BXD_11336	Male number of jumps 0-15min after injection
Chr14	107.221504	5.44	BXD_11356	Male number of beam breaks in an open field 0-15 min after injection
Chr14	107.221504	6.44	BXD_11357	Male horizontal activity (distance traveled) 0-15min after injection
Chr16	28.04168	8.41	BXD_11596	Female change in locomotion activity

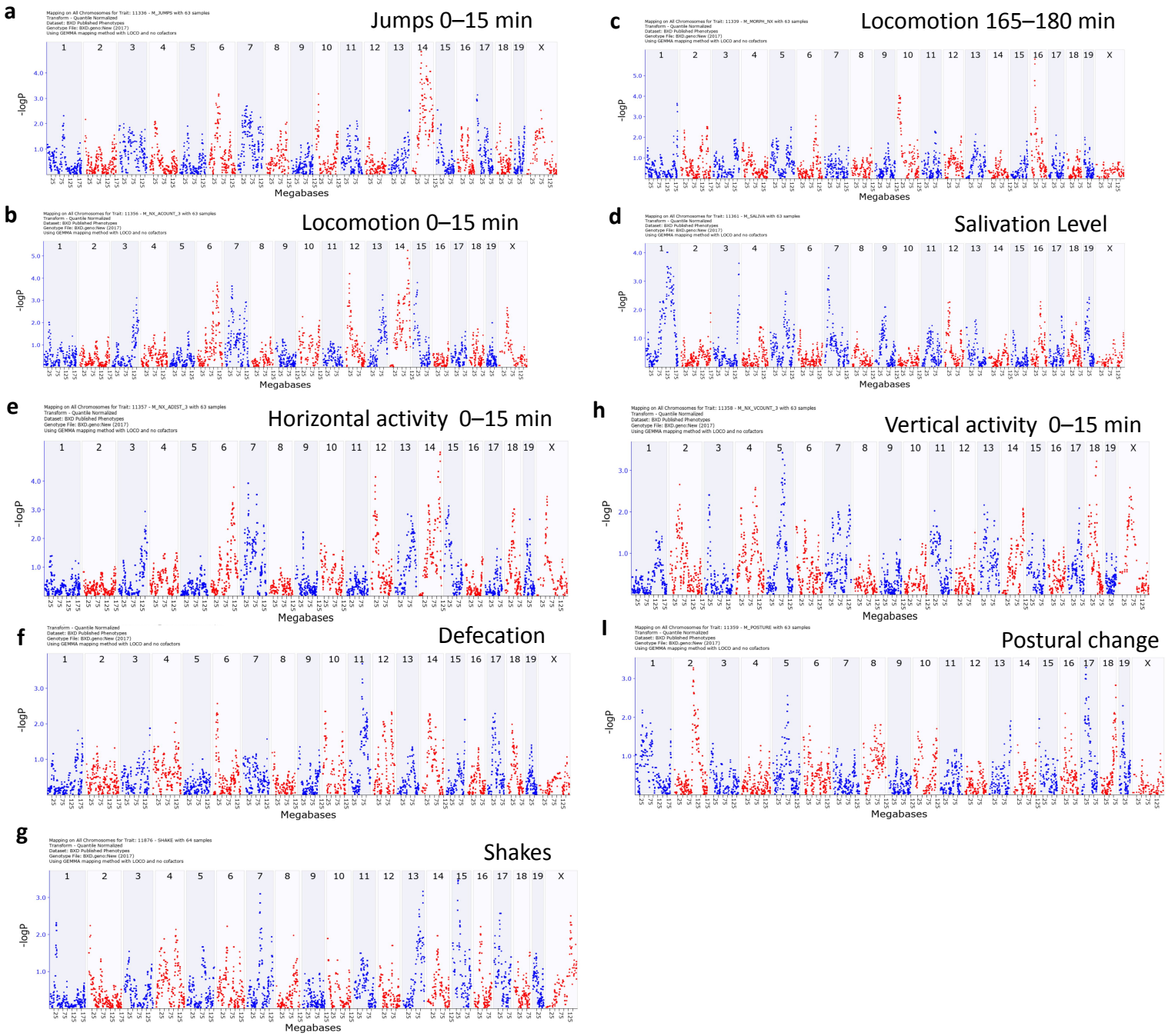

Figure 6: Male Naloxone-Induced Morphine Withdrawal Response QTL Maps

QTL of naloxone-Induced morphine withdrawal response in males. Arrow and star marks indicate the morphine locomotion peaks on chr 10 and 16. **(a)** Number of jumps 15 minutes after naloxone injection, with a –logP of 4.89 and a high B allele. **(b)** Number of beam breaks in an open field 0–15 min after naloxone injection. **(c)** Change in locomotion measured by the last 15 min of morphine locomotion response minus the first 15 min after naloxone injection. **(d)** Salivation level. **(e)** Horizontal activity (distance traveled) 0–15 min after naloxone injection. **(f)** Defecation in an activity chamber (number of fecal boli). **(g)** Wet dog shakes. **(h)** Vertical activity (rears) 0–15 min after naloxone injection measured by number of beam breaks. **(I)** Postural change.

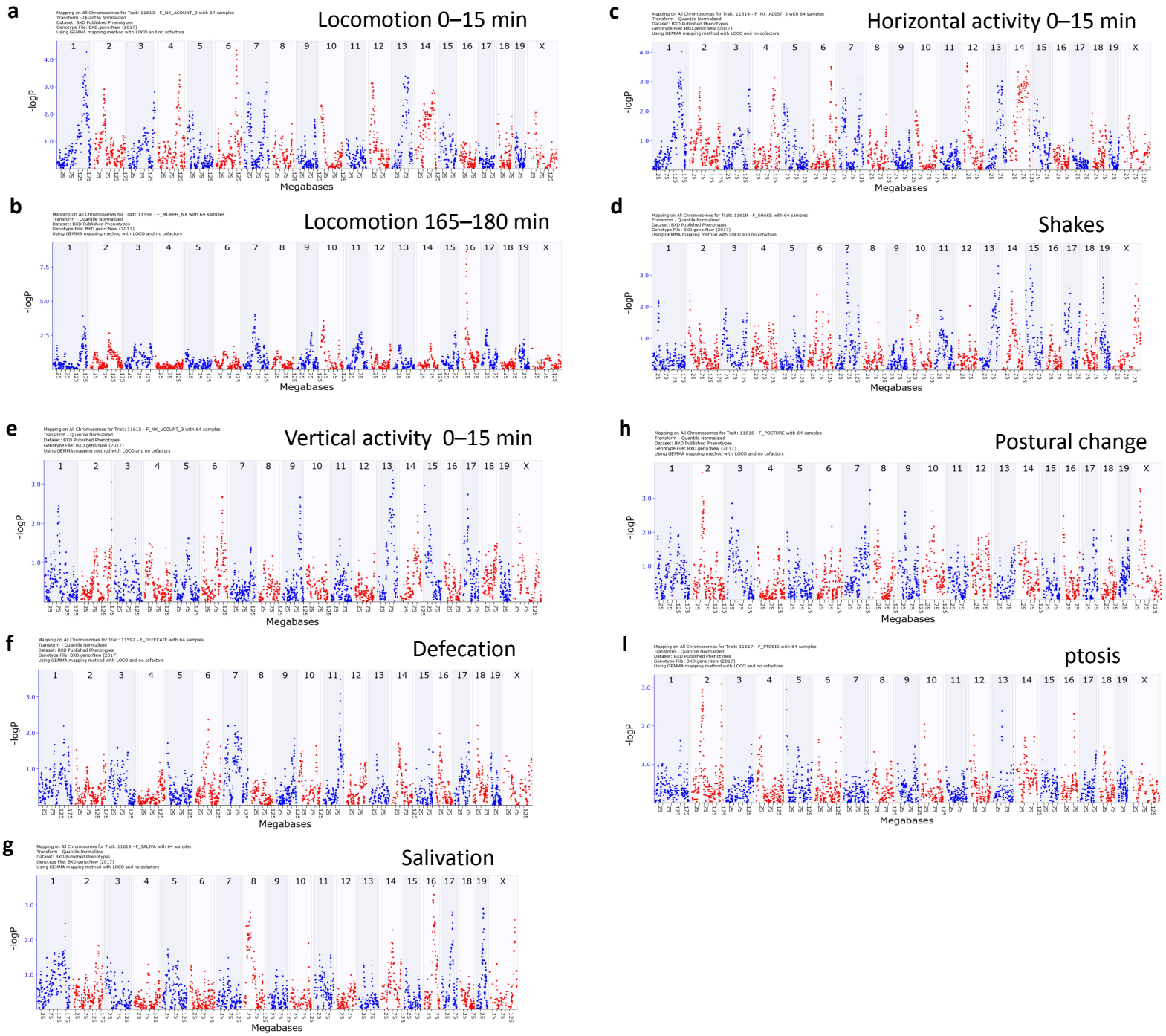

Figure 7: Female Naloxone-Induced Morphine Withdrawal Response QTL Maps

Female naloxone-induced Morphine withdrawal behavioral responses QTL maps. Arrow and star marks indicate the morphine locomotion peaks on chr 10 and 16. **(a)** Number of beam breaks during open field 0–15 min after naloxone injection. **(b)** Change in locomotion measured by the last 15 min of morphine locomotion response minus the first 15 min after naloxone injection. **(c)** Horizontal activity (distance traveled) 0–15 min after naloxone injection. **(d)** Wet dog shakes. **(e)** Vertical activity (rears) 0–15 min **(f)** Defecation in an activity chamber (number of fecal boli). **(g)** Salivation level. **(h)** Postural change. **(I)** ptosis.

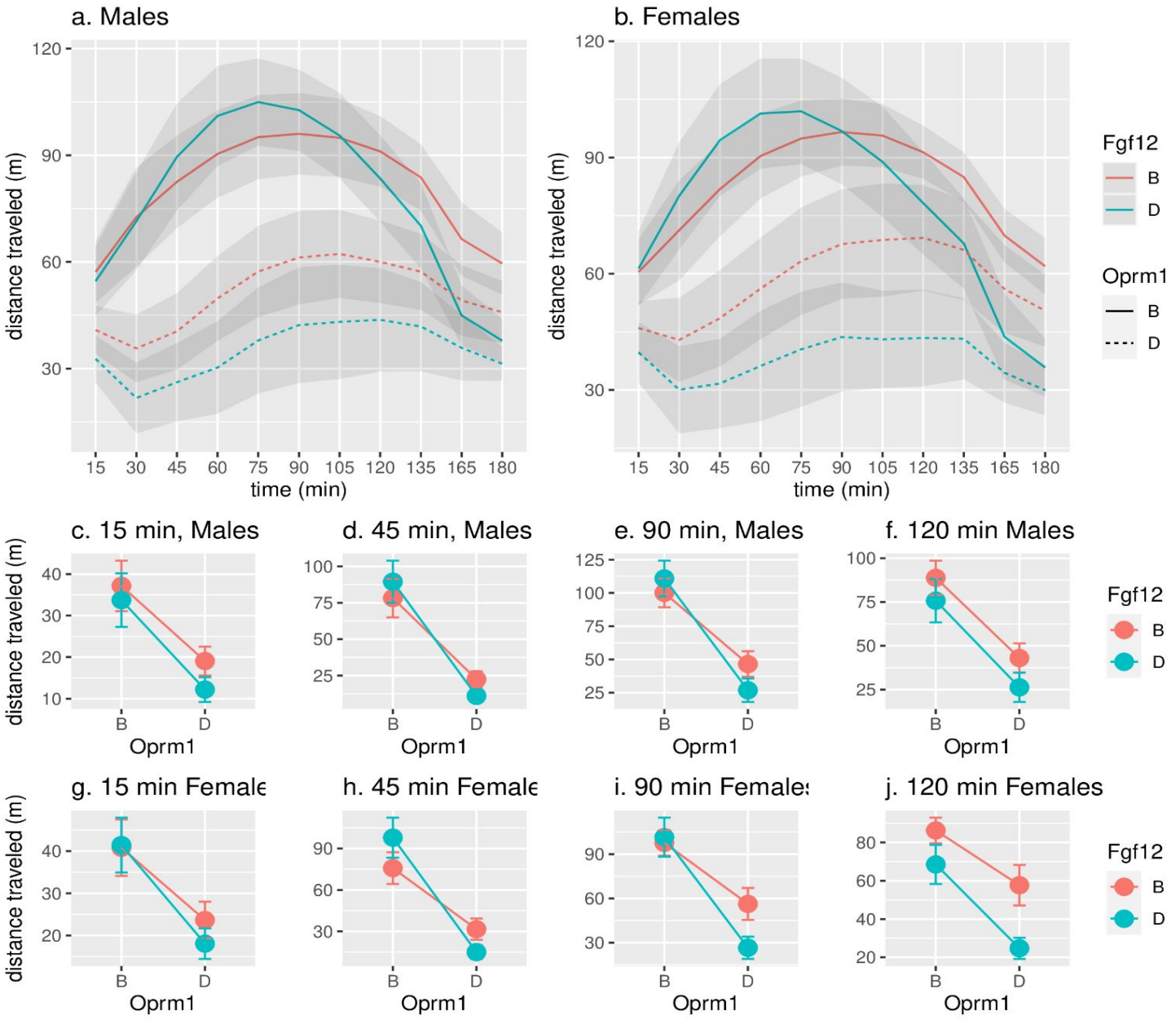

Figure 8: Epistatic Interaction Among Haplotype and Genotype Combinations

(a) Males and **(b)** females with different combinations of the "B" or "D" haplotype yield different phenotypic results for the distance traveled over time. Distance traveled (m) between the two genotypes in **(c-f)** males and **(g-j)** females.

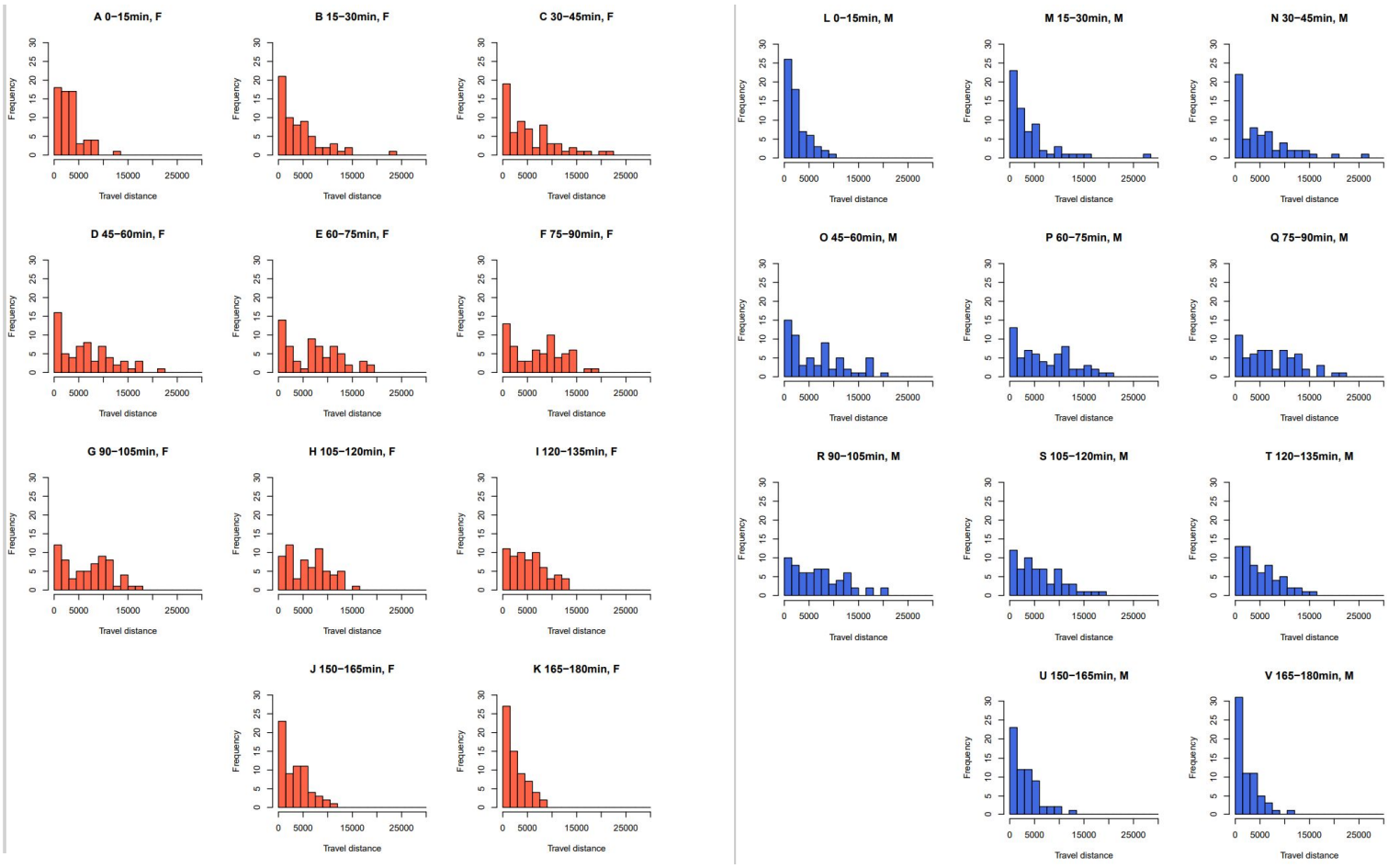

Supplemental Figure 1: Locomotion after Morphine Distribution Plots

Distribution plots of the raw data for locomotion after morphine injection, both females (orange **A-K**) and males (blue **L-V**).

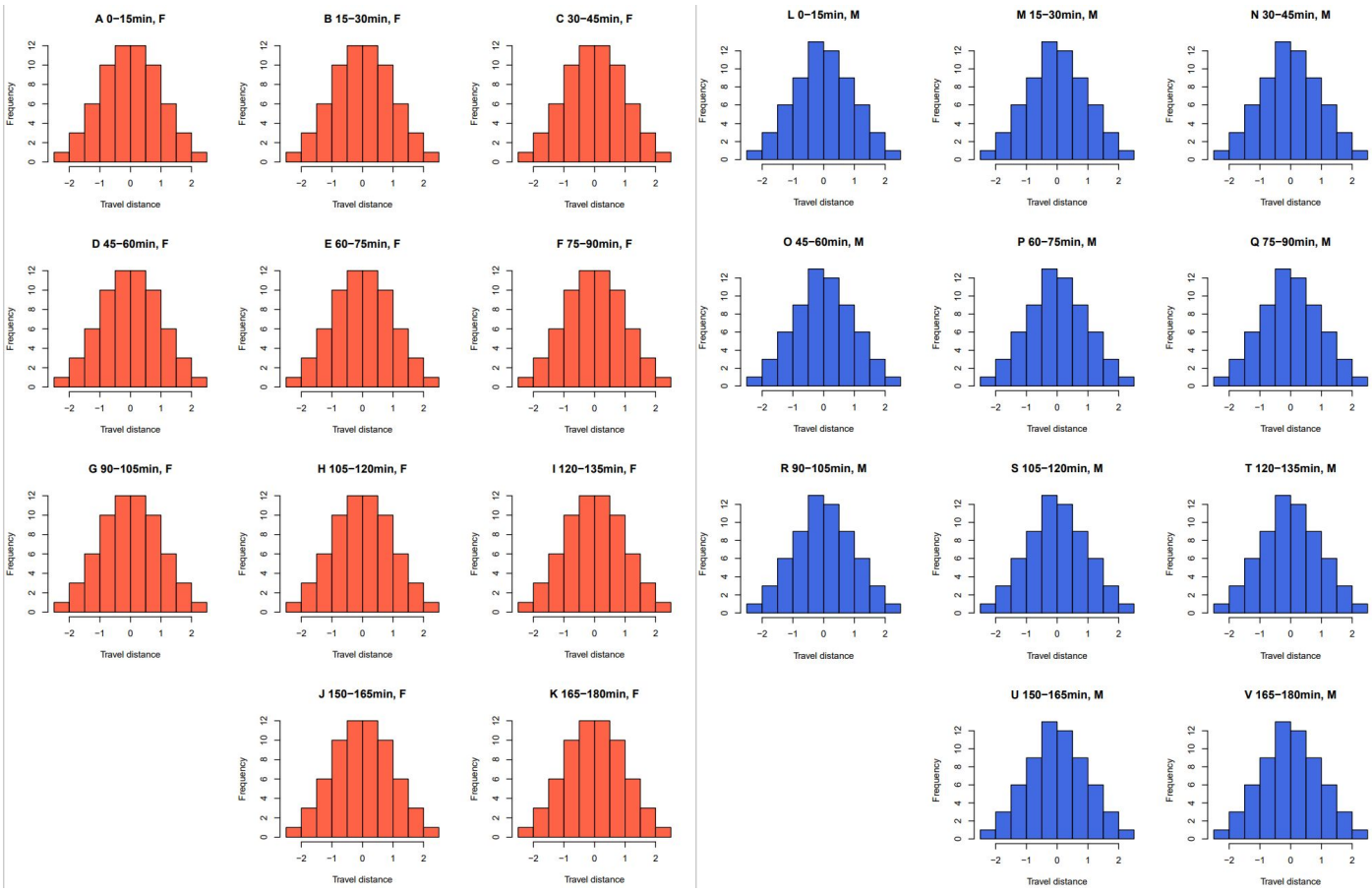

Supplemental Figure 2: Locomotion after Morphine Distribution Plots Quantile Normalized

Distribution plots of the quantile normalized data for locomotion after morphine injection, both females (orange **A-K**) and males (blue **L-V**).

Supplementary Table 3: Suggestive QTLs in Naloxone-Induced Withdrawal Behavior (Quantile Normalized)

Chromosome	Location (Mb)	-logP	Trait ID	Phenotype
Chr1	128.544902	4.3	BXD_11361	Male salivation level
Chr3	155.541974	3.82	BXD_11361	Male salivation level
Chr12	27.822843	4.2	BXD_11357	Male horizontal activity (distance traveled) 0-15min after injection
Chr11	77.010554	4.07	BXD_11335	Male defecation (number of fecal boli)
Chr13	110.44936	3.21	BXD_11876	Male wet dog shakes
Chr7	73.61994	3.52	BXD_11876	Male wet dog shakes
Chr15	32.696187	3.42	BXD_11876	Male wet dog shakes
Chr17	27.637041	3.03	BXD_11876	Male wet dog shakes
Chr18	54.61484	2.96	BXD_11358	Male vertical activity (rears) 0-15min after injection
Chr5	90.404862	3.57	BXD_11358	Male vertical activity (rears) 0-15min after injection
Chr17	31.615045	3.28	BXD_11359	Male postural change
Chr2	106.598183	3.65	BXD_11359	Male postural change
Chr6	117.480394	4.16	BXD_11613	Female number of beam breaks in an open field 0-15 min after injection
Chr1	170.535283	4.04	BXD_11613	Female number of beam breaks in an open field 0-15 min after injection
Chr13	69.104303	3.85	BXD_11613	Female number of beam breaks in an open field 0-15 min after injection
Chr6	117.480394	3.29	BXD_11614	Female horizontal activity (distance traveled) 0-15min after injection
Chr1	170.535283	3.72	BXD_11614	Female horizontal activity (distance traveled) 0-15min after injection
Chr12	26.307605	3.58	BXD_11614	Female horizontal activity (distance traveled) 0-15min after injection
Chr14	93.711205	3.37	BXD_11614	Female horizontal activity (distance traveled) 0-15min after injection
Chr13	69.104303	3.28	BXD_11614	Female horizontal activity (distance traveled) 0-15min after injection
Chr13	111.021029	3.35	BXD_11619	Female wet dog shakes
Chr7	73.61994	4.08	BXD_11619	Female wet dog shakes
Chr15	32.696187	3.24	BXD_11619	Female wet dog shakes
Chr15	3.977909	3.07	BXD_11615	Female vertical activity (rears) 0-15min after injection
Chr13	90.420704	3.34	BXD_11615	Female vertical activity (rears) 0-15min after injection
Chr17	27.637041	3.11	BXD_11615	Female vertical activity (rears) 0-15min after injection
Chr11	100.840973	3.47	BXD_11592	Female defecation (number of fecal boli)
Chr16	61.403305	3.54	BXD_11618	Female salivation level
Chr3	33.914701	3.21	BXD_11616	Female postural change
Chr7	144.447603	3.24	BXD_11616	Female postural change
Chr2	59.226414	3.15	BXD_11616	Female postural change
Chr2	173.549576	3.08	BXD_11617	Female ptosis

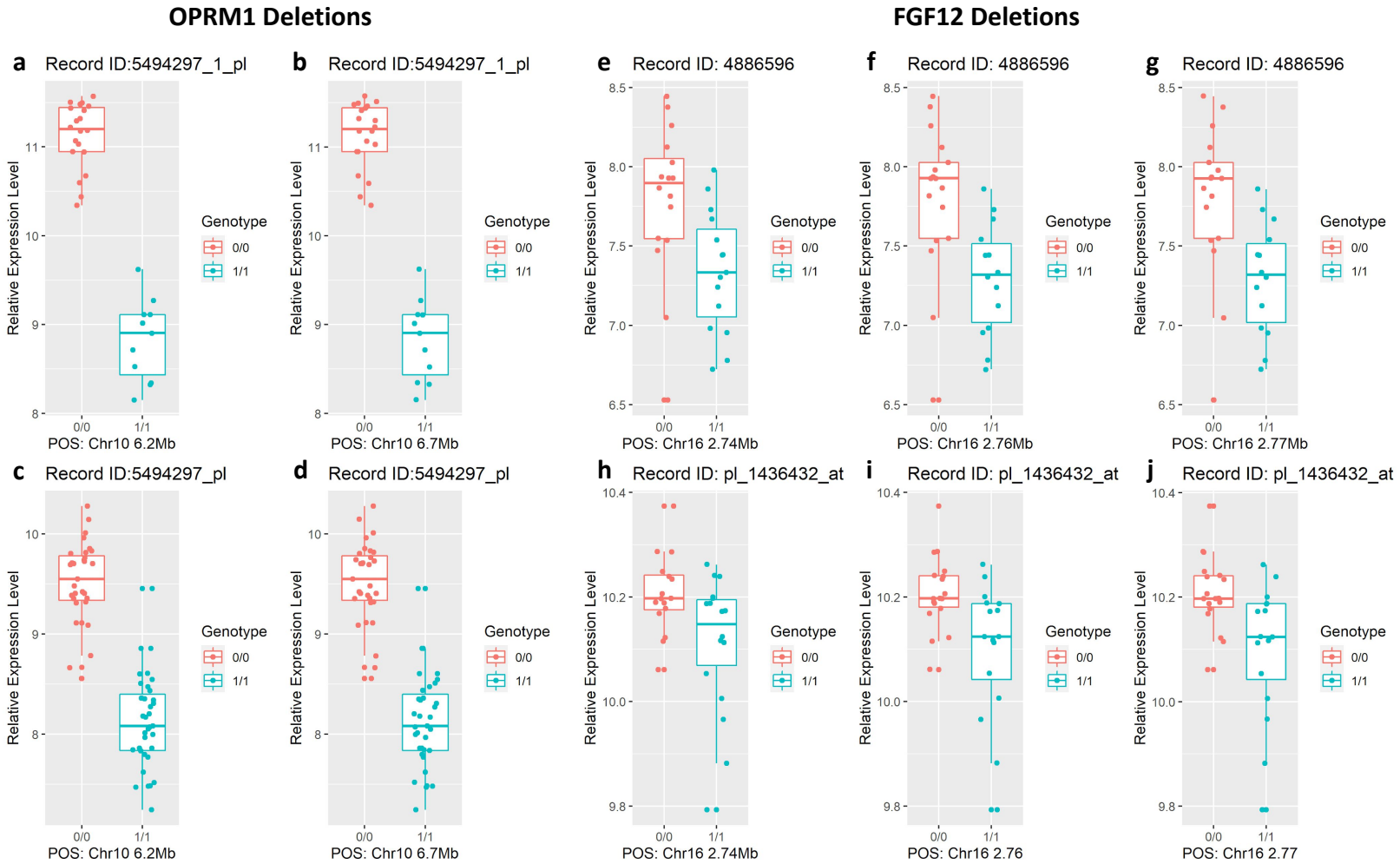

Supplemental Figure 3: Deletions Found in the 5' UTR Region of OPRM1 and FGF12

Two deletions found in the 5' UTR region of OPRM1 on Chr10 6.2Mb and 6.7Mb in BXD **(a-b)** striatum and **(c-d)** hippocampus. Three deletions found in the 5' UTR region of FGF12 on Chr16 2.74Mb, 2.76Mb and 2.77Mb in the BXD **(e-g)** VTA and **(h-j)** striatum. The x-axis is the genotype for the deletions. The y-axis is the relative mRNA expression level. The 0/0 reference genome indicates the expression level without the deletion (orange) and the 1/1 alternative indicates the expression level without the promoter region deletion (blue).

a

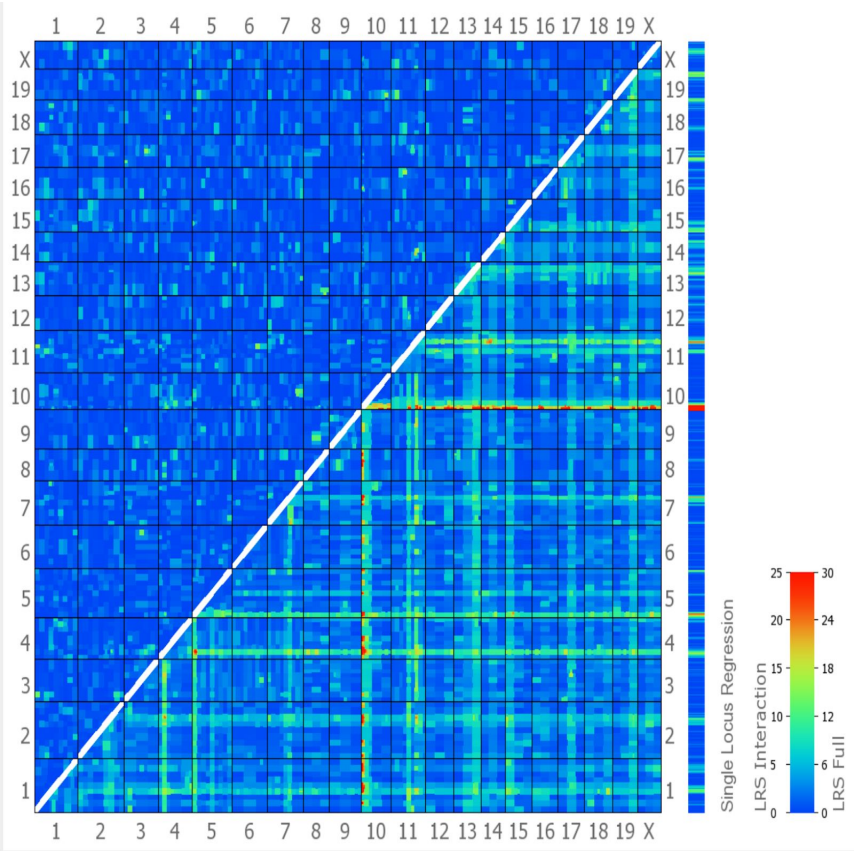

b

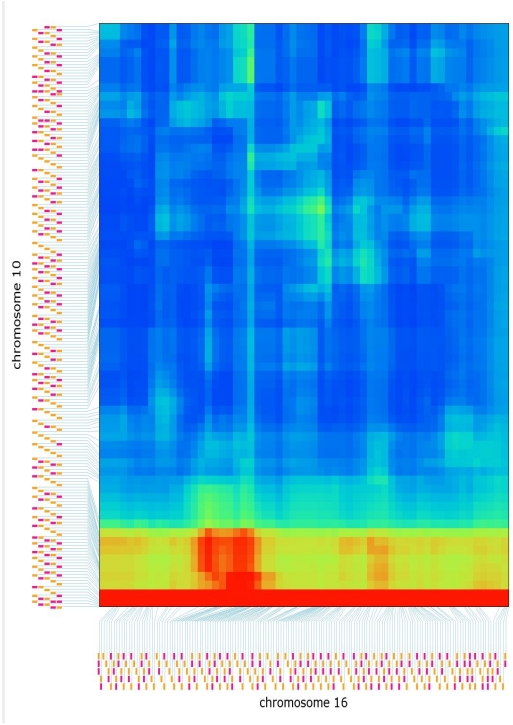

Supplemental Figure 4: Pair-wise Linkage Statistics Heat Map of Marker Combinations Across Genome

(a) The two-dimensional heat map of the linkage statistics shows all pair-wise combinations of markers across the genome—both additive effects and interaction effects. A conventional genome-wide scan of the main effect is shown graphically to the far right as a single separate column. The upper left side of the diagonal is color-coded for the epistatic interaction term in the statistical model. **(b)** One of the chromosome-chromosome intersection heat maps zoomed in. The bright red line along the bottom is the additive effect

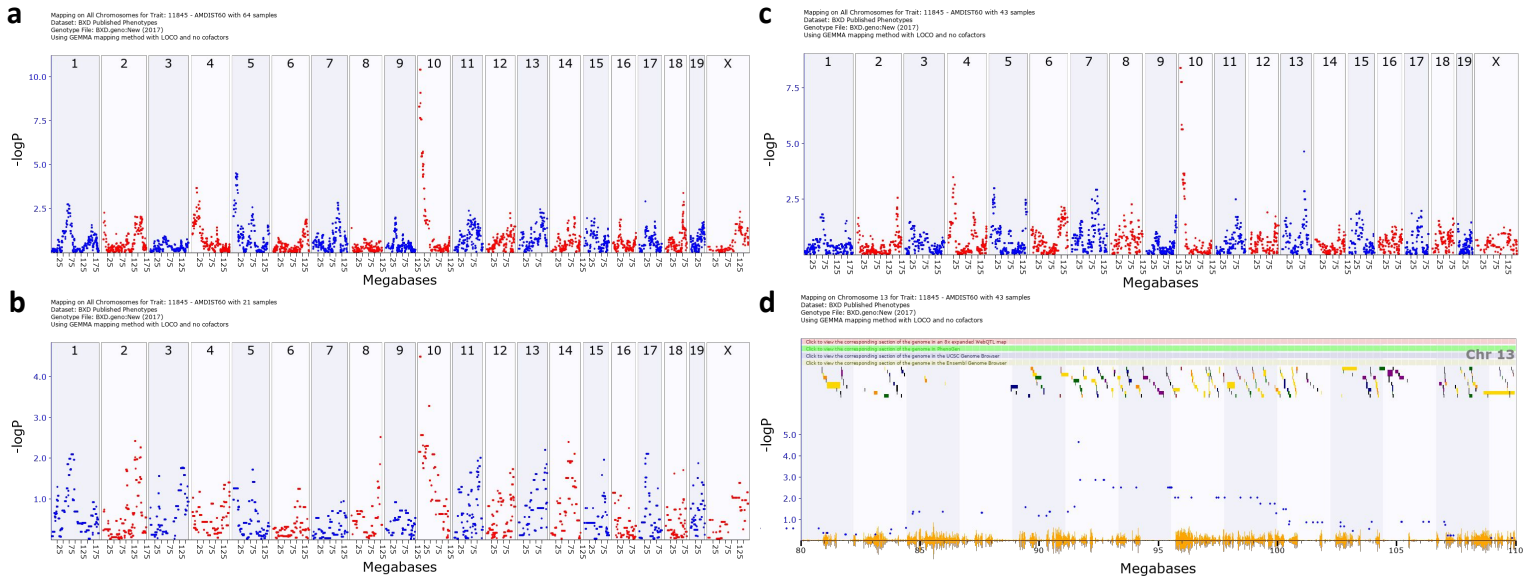

e

☐	54	A830009L08Rik	91.368989	19.096	54	2.827817	--	--	--	RIKEN cDNA A830009L08 gene
☑	55	Ssbp2	91.461096	211.312	160	0.757174	--	5	80.751427	single-stranded DNA binding protein 2
☐	56	AK039140	91.524584	1.423	1	0.702741	--	--	--	adult male hypothalamus cDNA, RIKEN full-length enriched library, clon...
☐	57	4833422C13Rik	91.701664	40.208	21	0.522284	--	--	--	RIKEN cDNA 4833422C13 gene
☑	58	Acot12	91.741520	44.628	37	0.829076	--	--	--	acyl-CoA thioesterase 12
☐	59	4933440K10Rik	91.780898	1.457	1	0.686342	--	--	--	RIKEN cDNA 4933440K10 gene
☐	60	Zcchc9	91.796532	11.164	32	2.866356	--	5	80.633177	zinc finger, CCHC domain containing 9
☑	61	Ckmt2	91.853386	23.499	58	2.468190	--	5	80.564937	creatine kinase, mitochondrial 2
☐	62	1700119I11Rik	91.861431	0.611	0	0	--	--	--	RIKEN cDNA 1700119I11 gene
☐	63	AK018965	91.861431	0.611	0	0	--	--	--	adult male testis cDNA, RIKEN full-length enriched library, clone:1700...
☑	64	Rasgrf2	91.880406	107.636	225	2.090379	--	5	80.292313	RAS protein-specific guanine nucleotide-releasing factor 2
☐	65	Msh3	92.211877	143.126	133	0.929251	--	5	79.986241	mutS homolog 3
☐	66	Dhfr	92.354782	34.271	46	1.342243	--	5	79.958449	dihydrofolate reductase

Supplemental Figure 5: Effect of BXD Epoch on Morphine Responses

(a) All Epochs (1,2,3). **(b)** Epoch 1, Trait 11845 (both sexes at 45–60 min), n = 20 strains—BXD1 to BXD32. **(c)** Epoch 3, Trait 11845 (both sexes at 45–60 min), n = 43 strains—BXD33 to BXD100. **(d)** Map of Chr 13 Trait 11845. **(e)** And the candidates in this interval of Chr 13.